Capturing Tactile Properties of Real Surfaces for Haptic Reproduction

Donald Degraen
donald.degraen@dfki.de
Saarland University & German Research Center for
Artificial Intelligence (DFKI), Saarland Informatics Campus
Saarbrücken, Germany

Michal Piovarči
michael.piovarci@ist.ac.at
Institute of Science and Technology Austria (IST Austria)
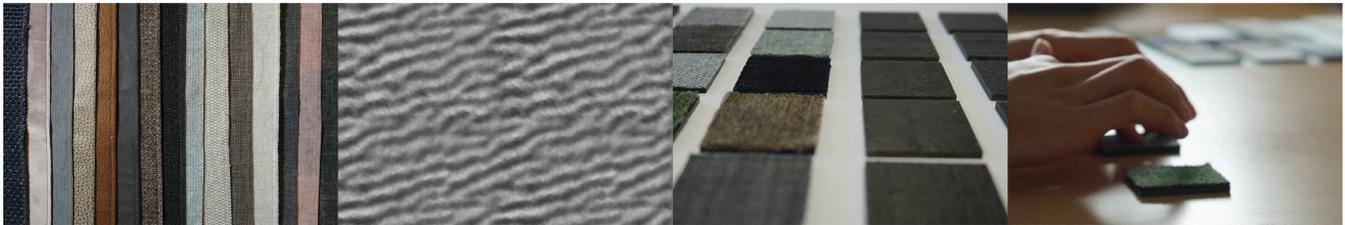Klosterneuburg, Austria

Bernd Bickel
bernd.bickel@ist.ac.at
Institute of Science and Technology Austria (IST Austria)
Klosterneuburg, Austria

Antonio Krüger
krueger@dfki.de
German Research Center for Artificial Intelligence (DFKI),
Saarland Informatics Campus
Saarbrücken, Germany

Figure 1: Overview of our approach. By reconstructing surface textures from a sample book using a photometric reconstruction method, we created fabricated replicas. The set of original and replica surface samples were used in a 2-part user study to investigate the transfer of tactile properties for additive manufacturing.

ABSTRACT

Tactile feedback of an object's surface enables us to discern its material properties and affordances. This understanding is used in digital fabrication processes by creating objects with high-resolution surface variations to influence a user's tactile perception. As the design of such surface haptics commonly relies on knowledge from real-life experiences, it is unclear how to adapt this information for digital design methods. In this work, we investigate replicating the haptics of real materials. Using an existing process for capturing an object's microgeometry, we digitize and reproduce the stable surface information of a set of 15 fabric samples. In a psychophysical experiment, we evaluate the tactile qualities of our set of original samples and their replicas. From our results, we see that direct reproduction of surface variations is able to influence different psychophysical dimensions of the tactile perception of surface textures. While the fabrication process did not preserve all properties, our approach underlines that replication of surface microgeometries benefits fabrication methods in terms of haptic perception by covering a large range of tactile variations. Moreover, by changing the surface structure of a single fabricated material, its material perception can be influenced. We conclude by proposing strategies for capturing and reproducing digitized textures to better resemble the perceived haptics of the originals.

CCS CONCEPTS

• **Human-centered computing** → **User studies**; *Haptic devices*; *Human computer interaction (HCI)*.

KEYWORDS

surface replication, texture perception, haptic feedback, digital fabrication

1 INTRODUCTION

The sense of touch is one of our most dominant senses. Through our fingers, we learn about the outside world [22] and perceive the properties of materials that allow us to perform fine control tasks [1, 16]. The ubiquitous nature of haptic feedback becomes most relevant during its absence. Without the sense of touch, we cannot tell if the clothes we wear are comfortable, and our fine

motor-control ability is greatly impaired even when directly observing our hands [58]. Therefore, during fabrication designers carefully need to select the haptics of surfaces to convey perceived quality and facilitate manipulation.

Manufacturing faithful tactile experiences is a challenging task. The haptic response of an object depends on its geometry, material, and the used manufacturing process which makes interactive editing of haptic response difficult. Without the option to freely alter the haptic feel of a digital design, designers usually resort to appropriating experiences from real-life by mimicking the haptics of materials they are intimately familiar with. This is commonly done by equipping the manufactured models with haptic textures from scanned or procedurally generated data sets [80]. It is unclear however if such visual representation can truly capture the haptics of a surface, nor how we can adapt it for different materials or manufacturing techniques. As a result, there is not yet an established framework for replicating the haptic properties of materials.

In this work, we investigate the replication of real-world information for the purpose of fabricating tactile variations. Rather than aiming for direct reproduction of tactile perception, we investigate the change in haptic properties upon replication. To this aim, we follow an end-to-end process. We start by capturing the haptic properties of materials, which we propose to do by reproducing their stable surface geometry. The geometry is captured using a photometric sensing technique called *GelSight* [33] as heightfields of surface samples. This approach works by pressing a soft polymer onto the material, similar to the investigation by direct touch. As a set of materials, we opted for a set of 15 cloth samples from a fabric samples book, depicted in the leftmost image in Figure 1. We opted for these challenging materials due to their large coverage of compliance, roughness, and friction properties, as well as their varying surface structures. To fabricate the materials we treat the captured heightmaps as displacement maps and use an Objet Connex 260 multi-jet printer with VeroBlack material.

In a psychophysical experiment, we assess the perception of the reproductions based on individually perceived attributes. From these results, we conclude that our fabrication process supports a wide gamut of *feel* aesthetics. While direct reproduction of surface geometry is not sufficient to consistently replicate the haptics of real-life materials, certain stable properties can still be reproduced to an extent. By further analyzing the results we discover that our reproductions manifest a consistent shift in perceived attributes. This suggests that the alteration of haptic feedback due to the selected fabrication technique is systematic and could be reversed by adjusting the printing parameters for our surfaces. Therefore, we propose a method to appropriate i.e., adapt, the haptic feedback of materials for digital fabrication. As a core of our approach, we construct a so-called perceptual space of our stimuli in which the perceived difference corresponds with measurable physical attributes. We leverage the perceptual space to propose several strategies for adapting material properties to more closely mimic their haptic properties after fabrication. Our results can provide insights for the field of haptic design by supporting hapticians in creating versatile haptic experiences through capturing real-world information for fabrication processes.

2 RELATED WORK

To appropriate haptic feedback perceived by our finger during active exploration, we draw inspiration from perception, surface reconstruction, and computational fabrication. Here, we provide an overview of work related to our approach.

2.1 Tactile Perception of Textures

The human finger has impressive discriminative power. During passive touch, our fingers can identify embossed dots down to 550 microns in diameter and a height of only 3 microns [85]. Our sensitivity to surface texture is increased during active exploration. The finger ridges interact with the underlying substrate and the resulting effect of pattern beating heightens our sensitivity which allows us to discriminate sinusoidal gratings down to 13 nanometers in height [68]. When continually exploring a surface formed of various bumps we perceive them as vibrations that are appreciable up to 500 Hz with the highest sensitivity around 240 Hz [32]. It is due to these capabilities at discriminating individual signals that faithful reproduction of haptics is an open and challenging problem.

The individual signals perceived through our fingertips are integrated into judgments of tactile properties [90]. To identify the governing phenomena Hollins et al. [27] conducted one of the first large scale studies with 17 tactile textures. They discovered that participants discriminate the samples based on perceived roughness, compliance, and stickiness. These findings were supported in subsequent studies [78] that also discovered additional dimensions for heat transfer [3, 9], and macro-roughness [46, 69]. Reproducing these perceived quantities is crucial in developing realistic virtual haptic experiences [14]. As a result, psychophysical models for comparing the governing perceptual attributes were developed [54, 55, 79, 81]. In contrast to previous work in perception, we aim to shed light on an open question of how to reproduce the haptic feedback of real textures using additive manufacturing where the smallest features are at the order of microns with a typical layer height of 10 micrometers [67]. To this end, we focus on identifying which perceptual cues are modified during 3D printing and propose a simple yet effective model to appropriate the haptic feedback of a digitized texture into the context of additive manufacturing.

2.2 Recording and Reproduction of Haptic Feedback

Humans rely on their sense of touch to explore materials based on various tactile cues. By collecting perceptually motivated cues such as hardness, roughness, macroscopic roughness, and friction it is possible to identify the material with a high degree of certainty [71]. Since many of these cues are coupled it is possible to encode them using the surface roughness [93]. The roughness can be captured via optical profilometers [13], mechanical probes [84], accelerometers [15, 25, 59], vision systems [30, 66], or specialty build sensors [49]. A particularly interesting approach is rethrographic sensing which is based on a transparent gel sensor covered by a diffusive film of known reflectance from one side [33]. To reconstruct the geometry the diffusive part is first pressed into the surface. This causes a deformation that can be measured through the clear side of the sensor with a camera using standard shape-from-shading techniques [95]. This approach can be further extended

to improve precision [34], or include additional measurements e.g. softness [94], applied force [20], or slip [92]. Moreover, recent work has detailed how portable approaches are able to serve in-the-wild capturing of surface features [42]. For a recent survey on tactile image sensing please see [65]. In this work, we build upon the rethrographic approach introduced by [34]. To reproduce the haptics of a surface we start by acquiring its geometry using a GelSight scanner and then manufacture replicas with a multi-jet printer.

The captured surface information can be used to replay the haptic feedback of materials. To reconstruct the haptic response it is possible to remodel the interaction in a virtual environment and then render the appropriate forces on a haptic device [38, 52, 83]. Unfortunately, numerical modeling of the coupled elastofrictional contact between a human finger and the underlying substrate is challenging at the rates required for haptic reproduction [41]. As a result, many data-driven models were considered [2, 8, 36, 43]. A particularly appealing option is to record the forces applied during interaction and replay them using a vibromotor [10, 48, 60, 77]. Such playback can be enhanced by rendering an infinite stochastic signal [24] and even adapted to the interaction speed and pressure [15, 45, 59]. However, the realism of the reproduced feedback via active modulation is significantly affected by the latency inherent to the systems [1, 7, 26]. Here, we focus on passively reproducing the tactile properties of a surface when explored by a bare finger.

2.3 Fabrication of Tactile Properties

Haptic feedback is a crucial asset in designing tangible virtual and real interfaces [5, 17, 58, 70]. Through the use of tactile information, we can enhance user interfaces to be both more intuitive and accessible. Over the years many methods were designed to provide tactual information. These methods range from passive, where the haptic information is encoded by using e.g., magnetic fields [86–89], surface texture [19, 31, 72, 73, 75, 76], or by creating hair-like structures [18, 40, 47], to active modulation mediated by vibratory signals [10, 36, 59], physical displacement [37, 52, 62], or electrical stimulation [2, 23]. However, designing effective haptic experiences remains a challenging task, partly because current design tools are missing support at different stages of the design process [35, 61, 64]. In this work, we wish to support the design of haptic experiences through appropriation of real world knowledge.

To fully appreciate an object it is important to faithfully reproduce its haptic feel. Torres et al. [80] proposed one of the first systems that allowed to design of objects' texture, compliance, and mass distribution. Since then more specialized methods were proposed to match the desired elastic behavior [44, 50, 63, 96], create functional cloth-like materials [29, 51, 56, 57, 74], and to mimic the haptic feedback of traditional drawing tools [53]. However, even with recent advances, there is no established method for the reproduction of haptic feedback experienced during active exploration with a finger. In this work, we tackle this open and challenging problem by investigating why directly manufacturing replicas of haptic feedback is challenging and by proposing several strategies to appropriate the haptics of materials in the context of additive manufacturing.

3 HAPTIC SURFACE REPLICATION

When exploring an object's surface, the high spatial acuity of our fingertips enables us to distinguish between the minuscule details in its texture. During this process, different aspects of the material are taken into account, most notably roughness, compliance, coldness, and slipperiness [3]. Of these features, related work has established roughness to be the most important for discrimination of haptically explored surface textures [4, 27, 28]. The perception of roughness is evoked by an uneven pressure distribution on the skin when touched statically, and vibrations when stroked. Physically, roughness is related to height differences on a material's surface.

We follow the idea that the geometric roughness of a surface can explain its tactile behavior. To reproduce the haptic feedback of real-life materials, we leverage the capabilities of modern manufacturing to reproduce the surface details at micron resolution. Recovering the surface information for fabrication requires a capture method that estimates the geometric features appreciated by an observer. During exploration, our fingers actively contact the underlying substrate which causes deformations of surface geometry. As a result, estimating the true stable contact requires a scanning method capable of inducing and measuring finger-like deformation of the original material.

3.1 Approach

Our implementation is based on retrographic sensing [34]. This approach also referred to as *GelSight*, employs a transparent elastomeric silicone coated with a layer of reflective paint of which the bidirectional reflectance distribution function (BDRF) is known. When pressing the silicone onto an object, the microscopic deformations of the reflective layer caused by the object's surface topography are made visible through the clear side of the sensor. By capturing the deformation under calibrated lighting conditions from different angles, the desired 3D shape and texture can be accurately reconstructed using a photometric stereo algorithm. This approach is highly flexible as the overall shape, thickness, and hardness of the *GelSight* sensor do not significantly affect the precision due to individual calibration [34, 65]. The only practical constraint is that the sensor needs to be sufficiently large enough to scan the area of interest.

This technique is closely related to the haptic exploration of surface textures with our fingers. While pressing down onto an object, stable surface features such as surface variations are perceived by the receptors in our fingers and unstable features such as hairs are compressed. Additionally, surface reconstruction with a calibrated sensor is possible using a single image capture while abstracting physical surface information from the visual appearance.

3.2 Surface Reconstruction

Building on the *GelSight* technique, we constructed a sensor, see Figure 2a, consisting of a hexagonal silicone slab measuring 1.5 cm in height and 8 cm in diameter. The clear silicone used has a Shore A hardness rating of 15[1] and was spray-painted with a layer of aluminum powder with a purity of 99.7% and a size of −325 mesh using a silicone paint base[2]. The reflective layer was powdered with

---

[1]KauPo Solaris® – www.kaupo.de
[2]Smooth-On PsychoPaint – www.smooth-on.com

(a) Silicone Sensor   **(b) Bench Setup**
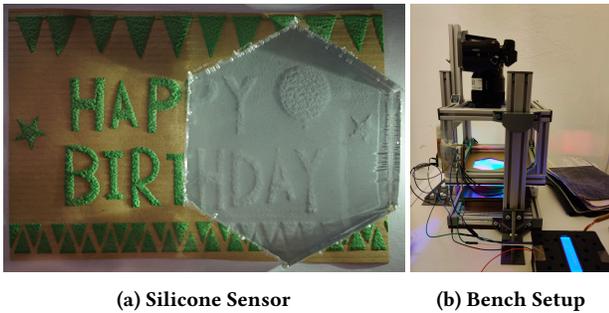
Figure 2: Our reconstruction setup. (a) A silicone slab with a reflective layer deforms and visualizes the surface texture of an object pressed underneath. (b) Using a bench setup, consistent captures are taken with a high resolution camera and a macro lens.

corn starch to reduce stickiness. To capture consistent images, we built a bench setup, see Figure 2b. Attached to the top of the setup is a Sony Alpha 7s full-frame DSLR camera with a Sony SEL FE 50 mm f2.8 macro lens. The camera is pointed towards the silicone sensor attached to a 2 mm transparent acrylic support. Driven by an Arduino Uno, 3 LEDs illuminate the sensor from different angles, each corresponding to a different base color, i.e., green, red and blue. The base of the setup contains a load cell measuring the applied pressure to the surface. The reconstruction process follows a photometric stereo algorithm to generate a heightfield from the object visible under the sensor. To calibrate our setup, we capture the sensor's deformation of a 4 mm spherical object in 36 locations across the image. For each surface texture to be reconstructed, 4 pictures of the sensor's deformation were taken with the texture in different locations and orientations. For more details on the reconstruction algorithm, please refer to [34].

For each recorded texture sample, the resulting heightfield corresponded to a surface area of $2.8 \, cm^2$ of the original texture. As we considered this surface area too small to be sufficiently explored by participants, we upscaled the surface area to a size of $5 \, cm^2$ using a blended texture tiling approach. Here, each heightfield was tiled in a 4×4 grid with a 10% gradually blended overlap. The vertices of a 5×5 plane were transformed along the Z-axis by using the associated heightfield as a displacement map in Blender[3]. The edges of the plane were extruded downwards along the Z-axis by a factor of 0.4 and a bottom face was generated to create a closed cuboid with the replicated texture on top. Our models were fabricated using an Objet Connex 260 printer with VeroBlack material and a layer resolution of 30 μm. VeroBlack is a rigid, durable and high resolution photo-polymer with a Shore Hardness of 83–86 (Scale D). A step-by-step overview of the reconstruction process is presented in Figure 3.

3.3 Textures

To study the human perception of materials we seek to construct a dataset that covers a wide variety of haptic properties. As we were interested in how physical features affect the perception after

[3]Blender, a free and open-source 3D creation suite – www.blender.org

Table 1: The physical measurements of our texture samples, taken from the set of original texture samples before reproduction to provide insights into their physical variations in terms of roughness, compliance and stickiness.

Sample	Name	Roughness (RMS)	Compliance (kg)	Stickiness (angle)
1	Casino	0.16259	2.82	16.5
2	Velvet	0.01412	1.03	28.0
3	Crown	0.07589	2.40	26.0
4	Havanna	0.06618	1.75	27.0
5	Deluxe	0.07799	2.00	22.0
6	Clash	0.03667	1.20	20.5
7	Cosy	0.09089	0.52	20.5
8	Florida	0.09807	1.38	14.5
9	Yelda	0.05816	2.03	19.0
10	Trend	0.06598	1.36	19.0
11	Onyx	0.15941	1.14	14.5
12	Cosmopolitan	0.04553	0.99	24.5
13	Easy Care	0.10260	3.75	19.5
14	Matrix	0.01632	3.15	22.0
15	Vintage	0.08882	0.72	15.5
	Mean	0.07728	1.75	20.6
	SD	0.04342	0.94	4.37

reconstruction, we explored a large assortment of materials with a high variety of characteristics. For our final set of reconstructed materials, we decided on 15 samples from a sample book for a commercially available sofa. These materials were found to have a large range of tactile properties and maintained a stable surface suitable for reconstruction.

After the reconstruction, physical measurements of the samples were taken to record their tactile properties of roughness, hardness, and slipperiness, see Table 1. The assessment of roughness was determined by calculating the root mean square of the reconstructed heightfield [6]. Hardness was measured by recording the indicated weight on a load cell when multiple stacked layers of the surface with a uniform height were compressed with a fixed displacement [50]. Lastly, we recorded the angle of inclination of which a fixed object on top of the surface would start a movement to assess slipperiness [39]. These data depicted in Table 1, underline the wide range of tactile properties present in samples.

To prepare the cloth samples for our study, we cut $5 \, cm^2$ rectangles from the bulk material and attached them to 2 mm acrylic plates of the same dimensions. The final set of samples and their heightfield reconstructions are depicted in Figure 4.

4 STUDY

To evaluate the haptic feedback of our original and reproduced textures we rely on psychophysical experiments grounded in literature [82]. More specifically, we conducted our user study in two phases: (A) a self-assessment test in which the participants compare the samples based on a set of perceptual attributes, and (B) a magnitude estimation study that recovers the differences between our stimuli in an unsupervised manner.
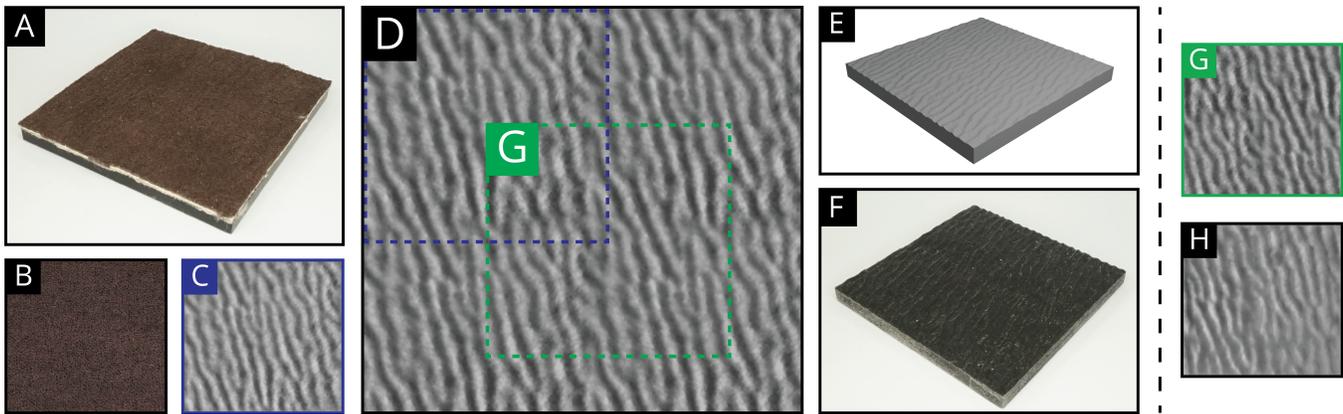
Figure 3: Reconstruction example. Visually capturing the texture surface (A) yields (B). The *GelSight* approach captures the stable subsurface geometry in a heightfield (C). From this information, we create a 5 cm² heightfield (D) using a combination of tiling and blending. The full heightfield is used as a displacement map to generate a textured surface (E), which is fabricated in (F). This process replicates the stable subsurface geometry of (A) in (F). For accuracy estimation, the fabricated sample (F) was re-reconstructed, i.e., here (G) is re-reconstructed in (H).
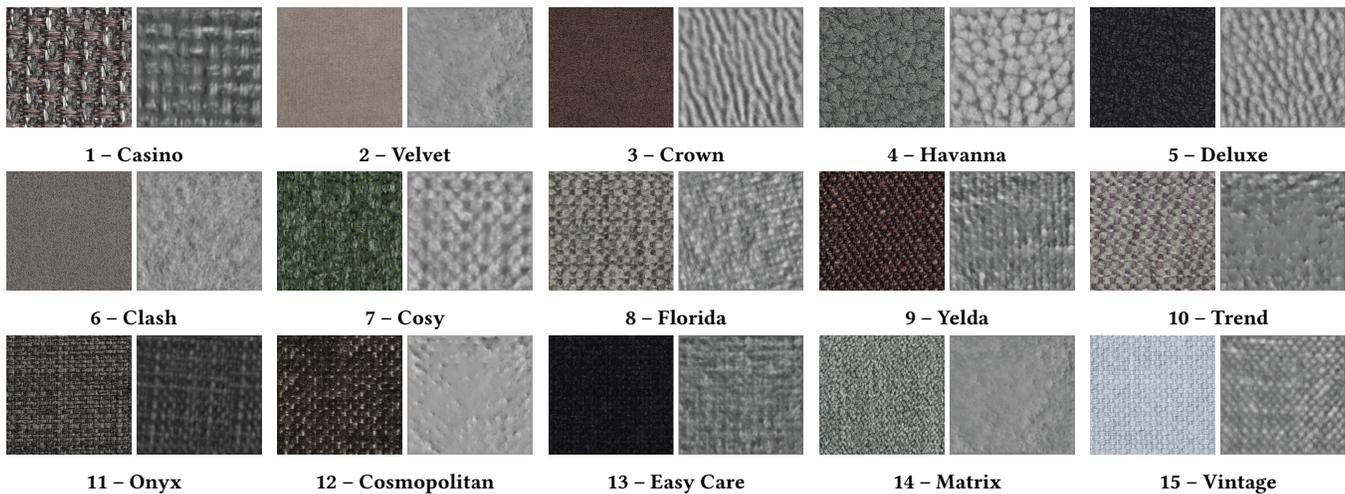
Figure 4: Our final set of surface textures and their reconstructed heightfields.

4.1 Apparatus

To limit visual cues, participants were seated in front of a screen separating them from the experimenter and the surface samples (Figure 5). A gap in the screen with a piece of cloth in front allowed the participants to reach their hand through to access the presented samples. On the other side, the experimenter prepared the samples for exploration by the participant. Samples were fixed in place using a laser cut MDF frame. The order of presentation of the samples was listed in a spreadsheet on a laptop next to the screen. Here, the experimenter would also record participants' answers.

4.2 Participants

A total of 20 participants (9 female, 11 male, 24 − 33 years, avg. 26.6 years) with backgrounds in Computer Science, Microbiology, Linguistics, and Law, were recruited for our study. When asked about their hand dominance, 19 participants indicated to be right-handed while 1 participant stated to be ambidextrous. All participants performed the study with the index finger of their right hand. Participants were informed that they could only use this finger.

All participants confirmed that, to the best of their knowledge, they did not suffer from any impairment of their haptic perception, such as arthritis or hypoesthesia (numbness). Participants rated on a scale from 1 (= never) to 5 (= regularly) how often they performed precise handwork ($M = 2.50$, $SD = 1.00$) and how frequently they worked with textiles ($M = 1.55$, $SD = 0.76$). The study lasted between 2 and 2.5 hours depending on the speed of the participant. Compensation in the equivalent of €20 was given to all participants not employed in our lab.

(a) The experimenter side **(b) The participant side**
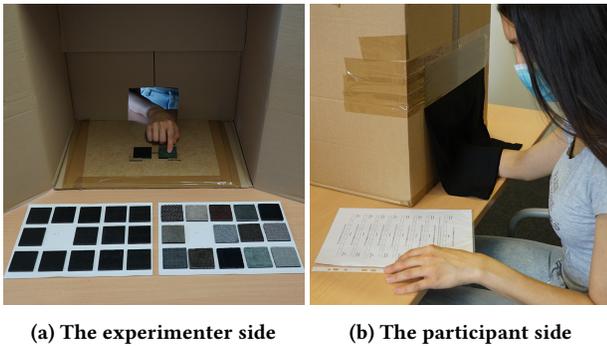
Figure 5: The experimental setup. (5a) The experimenter prepared the samples for exploration by the participant. (5b) The participant rated the tactile perception of the samples hidden behind the screen.

4.3 Procedure

Before starting the experiment, participants provided written consent and completed a COVID-19 form for contact tracing purposes. To comply with data protection regulations, the responses of the latter were removed 14 days after participation. The experimenter briefed participants on the upcoming events and asked them to seat themselves behind a separation screen.

After introducing the participants to the experimental conditions, we conducted a short training session. This training aimed to ensure understanding of the perceptual descriptors investigated in the study. Participants were presented with exemplar structures for each descriptor and asked to explore them under the experimental conditions. Once we were confident participants could identify the individual descriptors, we proceeded with the study itself.

Our study consisted of two phases, i.e., individual surface texture assessments (A), and surface texture similarity assessments (B). During phase A, the experimenter placed one of the surface samples on a fixed location behind the screen. The participant was then asked to explore the sample and rate various tactile properties of the sample one by one. During this phase, the participant was allowed to touch the sample continuously with the index finger of their dominant hand. The experimenter noted the responses for each trial and placed the next sample upon completion of the 9 questions. The following questions were depicted on a sheet of paper in front of the participant:

Q1: How **hard** does this surface feel? (1 meaning extremely soft, 9 meaning extremely hard)

Q2: How **rough** does this surface feel? (1 meaning extremely smooth, 9 meaning extremely rough)

Q3: How **bumpy** does this surface feel? (1 meaning extremely flat, 9 meaning extremely bumpy)

Q4: How **sticky** does this surface feel? (1 meaning extremely slippery, 9 meaning extremely sticky)

Q5: How **scratchy** does this surface feel? (1 meaning extremely dull, 9 meaning extremely scratchy)

Q6: How **hairy** does this surface feel? (1 meaning extremely clean, 9 meaning extremely hairy)

Q7: How **uniform** does this surface feel? (1 meaning extremely irregular, 9 meaning extremely uniform)

Q8: How **isotropic** does this surface feel? (1 meaning extremely anisotropic, 9 meaning extremely isotropic)

Q9: What kind of **material** is this? (Open question)

During phase B, the experimenter placed two surface samples behind the screen on fixed locations next to each other. The participant was then asked to explore both samples and rate the similarity of the tactile sensations on a 9-point scale, where 1 meant both samples were extremely dissimilar, i.e., opposites, and 9 meant both samples were extremely similar, i.e., identical. To improve consistency, participants were only allowed to use the tip of their index finger on their dominant hand to interact with the samples. The interaction window was limited to 5 seconds per sample to ensure participants' first impressions were communicated to the experimenter, and to limit the study duration. Within this time, there were no limitations on the interaction mode. Participants were allowed to stroke the samples in arbitrary patterns and lightly press or tap the samples to assess their hardness. The experimenter noted the response for each trial and placed the next samples upon completion of the similarity question.

Breaks were issued between phases, every 100 assessments, or when the participant noted a feeling of numbness in their finger. In terms of COVID-19, windows were opened to air the room at regular intervals, both the experimenter and the participant wore masks, and the setup and all samples were disinfected between participants. After the experiment, participants completed a post-study questionnaire inquiring about their demographics.

4.4 Design

We used a within-subjects experimental design with a total set of 30 samples, consisting of 15 real surface textures and their 15 replicated counterparts. In order to counterbalance both study phases for carry-over effects, participants were assigned sequence numbers. Each evenly numbered participant started with phase A, while each unevenly numbered participant first performed phase B.

For phase A, we considered the presented sample as the independent variable and distinguish 9 dependent variables, i.e., the participants' tactile impressions of a sample in terms of hardness, roughness, bumpiness, stickiness, scratchiness, hairiness, uniformity, and to which degree the surface geometry of the sample felt isotropic, each on a 1-to-9 Likert scale, 1 indicating a low assessment and 9 indicating a high assessment of the respective variable. We chose compliance, roughness, and stickiness since they are considered the base of tactile exploration models [27, 28, 46, 82, 91]. The inclusion of bumpiness and scratchiness is motivated by [46] where the authors show that roughness can be divided into two dimensions for macro and micro roughness. The inclusion of hairiness, uniformity, and isotropy was motivated by the fact that our original set of textures were fabric samples. As hairs are inherent to them, their lack in the set of replicated structures would show correlations to other perceptions, specifically uniformity and isotropy as the

directionality given by the sensing of hairs could influence these factors. The last dependent measure was the open answer in which participants stated which material they thought to experience. For this open question, participants were not provided a list of materials to choose from but were free to provide any answer they saw fit. For counterbalancing measures, we constructed experimental design tables using a 30×30 Latin square. Here, counter-balancing was incomplete as the Latin square was performed for 20 rows, i.e., one row per participant.

For phase B, we distinguish the independent variable as the combination of samples presented to the user. Each participant was presented with all 435 possible combinations of our 30 samples. The order of sample presentation was randomized while the relative location of the presented sample for a given combination was alternated between participants. This meant that for a given combination, a sample was presented on the left side for an evenly numbered participant and on the right side of an unevenly numbered participant.

Ethical approval for this study was obtained from the Ethical Review Board of the Department of Computer Sciences at Saarland University (No. 20-07-2).

5 RESULTS

In the following section, we describe the analysis and the obtained results from our texture perception study.

5.1 Individual Tactile Ratings

To analyze the individual tactile assessments, we conducted Friedman tests with posthoc analysis using Wilcoxon signed ranks tests and Bonferroni-Holm correction for all comparisons. For completeness, all results are depicted in Appendix A. The ratings per sample for each case are depicted in Figure 6. Here, we focus our results on the patterns that arise in the analysis, specifically for the results within the set of original texture samples (T), within the set of replicated surface samples (R), and their cross-comparison for the same surface texture (T-R).

Hardness. The ratings of hardness were found to significantly differ depending on the sample ($\chi^2(29) = 445.83, p < .001$). Overall, the average ratings for the T samples ($M = 4.10$) were found to be lower than the average ratings for the R samples ($M = 7.95$). From our results, we could verify that the original set of samples consisted of surfaces with differing degrees of hardness. In contrast, the replicated samples were rated consistently high in terms of hardness. While this caused most original samples to differ from their replicas significantly, some similarities remained. The hardness of rough samples did not significantly differ between the original samples and their replicas. This effect was most notable for $T_{15\text{-vintage}}$. From these observations, we can conclude that the surface replication process affected the tactile perception of hardness.

Roughness. The ratings of roughness were found to significantly differ depending on the sample ($\chi^2(29) = 382.29, p < .001$). In terms of roughness, the T samples' average ratings ($M = 4.26$) were found to be lower than the R samples ($M = 6.82$). Differences in perceived roughness were significant in both original and replicated samples.

While the general trend indicates an increase in tactile roughness after replication, the replication process created a varying set of replicas by partly translating the roughness gamut. Cross-comparisons between all T and R samples indicated that 9 of our surface samples showed roughness to significantly increase from their original counterpart, while 6 samples preserved their level of roughness.

Bumpiness. The ratings of bumpiness were found to significantly differ depending on the sample ($\chi^2(29) = 393.01, p < .001$). The average ratings for the T samples ($M = 3.19$) were found to be lower than those of the R samples ($M = 6.14$). Similar to the results of perceived roughness, the ratings of bumpiness indicate differences within the original samples' set and within the set of replicated samples. The general trend indicates an increase in tactile bumpiness, while some variance was preserved after replication. Cross-comparisons between all T and R samples indicated 6 samples preserved their level of bumpiness.

Stickiness. The ratings of stickiness were found to significantly differ depending on the sample ($\chi^2(29) = 172.08, p < .001$). The average rating of the T samples ($M = 3.18$) was lower than the R samples ($M = 4.92$). Pair-wise analysis within the set of T samples and within the set of R samples indicated no significant differences. Cross-comparison between T and R samples revealed that only $T_{2\text{-velvet}}$ significantly differed from its replica. Here, we note that both our original and replicated samples were found to be mostly neutral in terms of stickiness, and the replication process did not alter its perception.

Scratchiness. The ratings of scratchiness were found to significantly differ depending on the sample ($\chi^2(29) = 315.01, p < .001$). In terms of scratchiness, the T samples' average rating ($M = 3.11$) was lower than the R samples ($M = 4.91$). Both within the set of original samples and the set of replicated samples, differences in perceived scratchiness were significant. While the general trend indicates an increase in tactile scratchiness after replication, the replication process created a varying set of replicas by partly translating the gamut of scratchiness. Cross-comparisons between all T and R samples indicated that only 5 of our surface samples showed scratchiness to differ from their original counterpart significantly; meanwhile, 10 samples preserved their level of scratchiness.

Hairiness. The ratings of hairiness were found to significantly differ depending on the sample ($\chi^2(29) = 394.38, p < .001$). The average rating of hairs on the replicated samples was lower than those of the T samples (T, $M = 5.63$; R, $M = 1.78$). For some T samples, the presence of hairs was significantly apparent compared to other T samples. As expected, in between all replicated samples, no significant differences were found for all combinations. For the cross-comparison between T and R samples, we note that the R samples were significantly different from most T samples, excluding those with a low hair presence. These results show that participants noticed the lack of hairs on the replicated samples.

Uniformity. The ratings of uniformity were found to significantly differ depending on the sample ($\chi^2(29) = 329.88, p < .001$). On average, the T samples' ratings ($M = 7.15$) were higher than the set of R samples ($M = 3.91$). While some significant differences were found within the original sample set, no differences were found
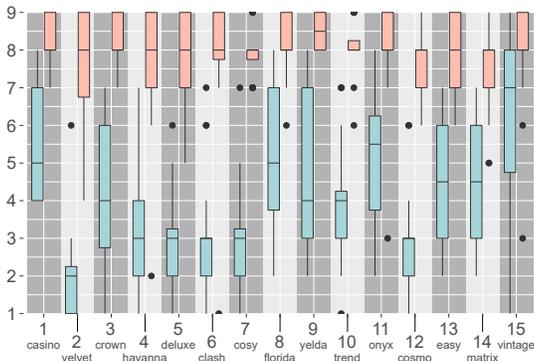
(a) Hardness.
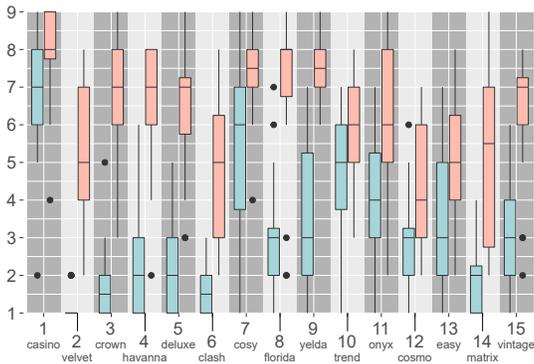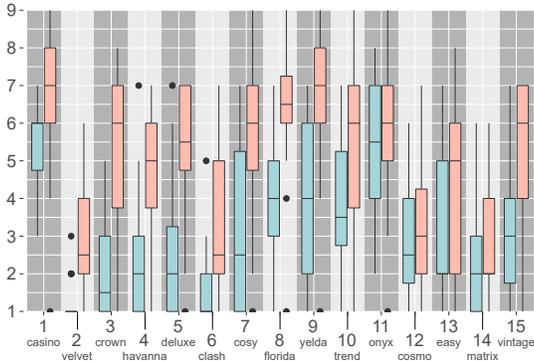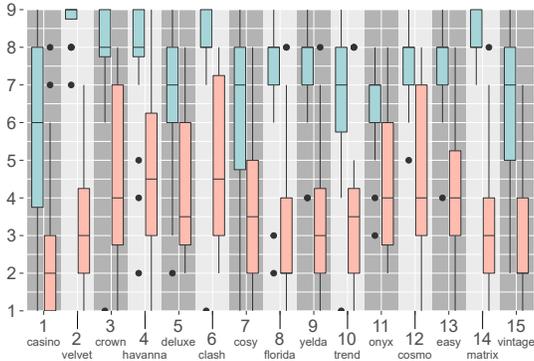
(b) Roughness.

(c) Bumpiness.

(d) Stickiness.

(e) Scratchiness.

(f) Hairiness.

(g) Uniformity.
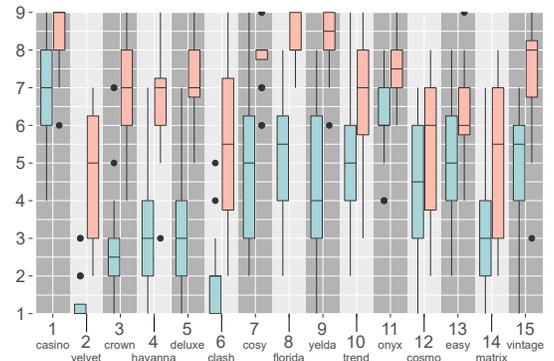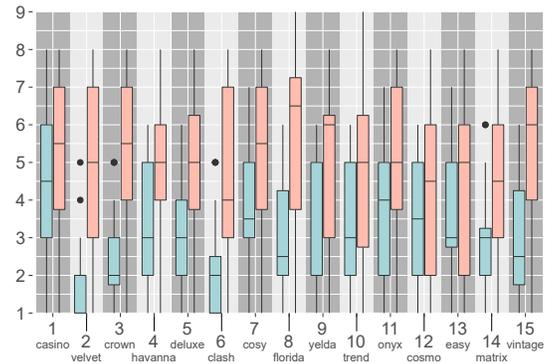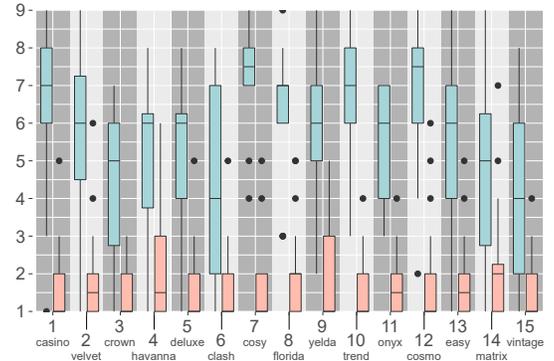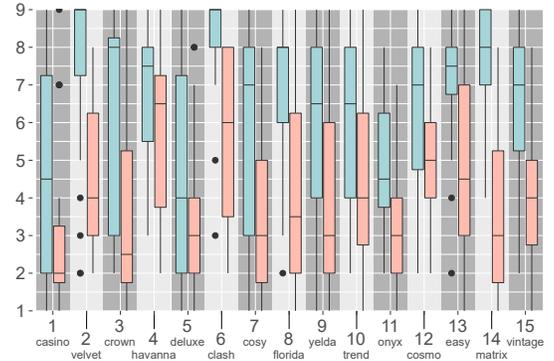
(h) Isotropy.

Figure 6: Boxplots indicating the individual assessments for each sample.
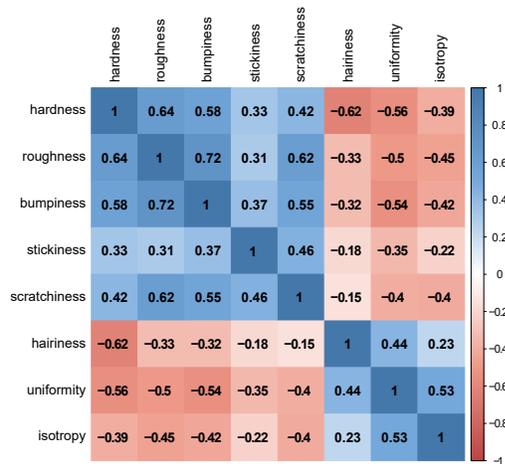
Figure 7: Correlation plot for the individual assessments. The numbers depict the Spearman's rank order coefficient (R_s). All correlations were found to be significant ($p < .01$).

within the set of replicas. Cross-comparison for the same texture showed 6 samples preserved their uniformity while 9 did not. From this, we see that the replication process lowered some indications of uniformity.

Isotropy. The ratings of isotropy were found to significantly differ depending on the sample ($\chi^2(29) = 189.08$, $p < .001$). When rating the uniformity in all orientations, participants noted higher isotropy for the original samples (T, $M = 6.33$; R, $M = 4.20$). Only three comparisons showed significant differences for all T samples, while for all R samples, no significant differences occurred. When comparing T samples to their partnered R samples, only $T_{6\text{-clash}}$ and $T_{14\text{-matrix}}$ did not preserve their level of isotropy. These results indicate that the replication process did not significantly alter the perceived isotropy for 13 samples.

5.2 Tactile Correlations

Using a Spearman's rank-order correlation, we found significant correlations between the different tactile assessments provided by participants. All correlations with their Spearman's rank order coefficients (R_s) are depicted in Figure 7. Here, all correlations were found to be significant ($p < .01$).

Strong positive correlations were found between the tactile ratings of roughness, bumpiness, and scratchiness. These observations were confirmed by the fact that participants noted it was sometimes difficult to distinguish between the individual features. The hardness of our samples is with varying effects positively correlated with the roughness, bumpiness, and scratchiness assessments. Interestingly, while hairiness is negatively correlated with hardness it has almost no effect on roughness, bumpiness, or stickiness. Two groups of tactile properties are appearing with opposite correlations with each other. While hairiness, uniformity, and isotropy are positively correlated with varying effect sizes, they are negatively correlated to the other tactile ratings.

(a) Stress plot. (b) Shepard diagram.
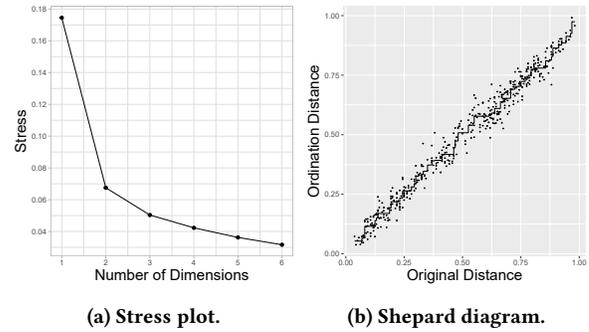
Figure 8: NMDS analysis. Here, 8a depicts the stress values for solutions using 1 to 6 dimensions, while 8b visualizes the relationship between the original and the ordination distances for a 3-dimensional solution.

5.3 Material Perceptions

The anecdotal data of the perceived materials were further analyzed by manually extracting the materials and objects identified by the participants. For the R samples, we characterized a set of 12 distinct perceived categories, namely *plastic-like* (28%), *stone-like* (27%), *wood-like* (27%), *fabric-like* (3%), *paper-like* (2%), *rubber-like* (2%), and *other* (4%, e.g., soap, dry glue, rough human skin, a surface with Braille, plastic made to feel like wood). For the T samples, we characterized a set of 9 distinct perceived categories, namely *fabric-like* (77%), *hair-like* (6%), *sponge-like* (6%), *leather-like* (6%), *rubber-like* (6%), *plastic-like* (6%), *paper-like* (6%), *stone-like* (6%), and *other* (6%, e.g., skin, mouse pad, feather, car ceiling). Within the category of *fabric-like* of the latter, we noted 10 recurring indications across participants, i.e., carpet, cloth, clothing, velvet, cotton, wool, felt, fleece, generic fabric, and others (fibers, linen, couch, curtain, and pillow).

5.4 Analysis of Similarities

To determine consistency across participants, we used Spearman's rank correlation tests on the similarity assessments. Here, we found the similarity ratings for each participant to be highly correlated with those of every other participant ($M_r = 0.69$, $p < .01$). Given this result, we note that participants rated the similarity assessments consistently.

For further analysis, the similarity assessments (1–9) were converted to normalized dissimilarity ratings (0–1). With these ratings, we created a symmetric dissimilarity matrix containing the perceptual distances between all original and replicated samples. Using an analysis of similarities, we compared different groupings within our distance matrix. We found a significant difference when comparing groups of the different sample types, i.e., original textures and replicated samples ($R = 0.9528$, $p < 0.001$). However, we did not find a significant difference when comparing groups of different sample numbers, i.e., all different sets of textures ($R = -0.3456$, $p = 0.99$).

5.5 Perceptual Space

For rating perceived similarity between two samples, participants were asked to consider all aspects of the tactile perception as they

saw fit. This instruction was given in order to not bias the judgments and acquire the true similarity assessments between our samples.

Analogous to literature [82], we used the obtained symmetric dissimilarity matrix to perform a non-Metric Multi-Dimensional Scaling (NMDS) analysis. NMDS is an indirect gradient analysis approach which produces an ordination based on a distance or dissimilarity matrix. When dealing with human similarity data, such an approach is common for calculating and visualizing perceptual spaces of the distances [12, 15, 82]. To understand how many axes are sufficient to visualize the perceptual space, we calculated the stress values for the first 6 dimensions, see Figure 8a. Here, the stress value of 0.05 for 3 dimensions approaches a faithful representation with no prospect of misinterpretation [11]. The low-stress level is underlined by the relationship between the original and ordination distances in Figure 8b.

Using Kruskal's non-metric multidimensional scaling approach, we then generated the perceptual space for our recorded assessments. In the resulting representation, the axes are unknown combinations as they do not represent apparent tactile assessments. To better understand the relationship between samples, we first build a physical space for the original texture samples. To this end, we build upon the previous work and use the 3 dominant dimensions of the tactile perception of surfaces, i.e., hardness, roughness, and stickiness [14, 91]. For each dimension, we use the z-scores of the respective recorded physical values for roughness, hardness and slipperiness, see subsection 3.2.

Using a Procrustean randomization test, we calculated the goodness of fit and its significance between the dissimilarity space of the original samples and the physical space ($m^2 = 0.65$, $p < 0.01$), between the dissimilarity space of the replicated samples and the physical space ($m^2 = 0.64$, $p < 0.01$), and between the dissimilarity space of the replicated samples and the original samples ($m^2 = 0.57$, $p < 0.01$). These results indicate that all data sets exhibit greater concordance than expected at random, indicating an agreement between the measurements obtained. Next, we performed a Procrustes analysis to calculate the transformation function from the physical space to the original sample's dissimilarity space such that they are in a state of maximal superimposition ($ss = 0.64$). The resulting rotation, translation, and scaling matrices were used to transform the physical space onto the perceptual space. Here, we included the physical's space axis as vectors in the transformation and label them according to their metrics. We depict the final perceptual space using 3 individual plots per dimension combination, see Figure 9.

6 DISCUSSION

Motivated by the recent advancements in the field of fabrication, we replicated a set of 15 texture samples by capturing and reconstructing their heightfields. Rather than aiming for direct reproduction of tactile perception, we investigate how the fabrication process affects the perceived haptic properties. We frame our discussion in two parts by first elaborating on the obtained results and their interpretations and providing insights for the fabrication of haptic properties.

6.1 Surface Haptics Appropriation

We aimed to determine how our approach influenced tactile surface properties' perception and gain insights into the relationship between the replication method and material perceptions. As we expected to see interactions between the original samples' tactile features and the perception of their replicated counterparts, we performed a psychophysical user study to understand these relationships. Here, we discuss our results that indicate our approach is an initial step for appropriating surface haptics and propose strategies for fabricating tactile properties.

Does surface geometry replication reproduce aspects of its feeling? The individual assessment results reveal that our set of original textures manifests significant variations in all observed tactile properties across samples. While many of the tactile variations of the set of replicated surfaces were compressed into smaller ranges, the replicas still indicated a degree of diversity. Therefore, appropriating tactile features from a diverse set of natural surfaces can provide an attractive solution for creating diverse haptic impressions on fabricated objects.

When comparing the original textures to their replicas, we observe that the printed materials do not maintain all the original materials' tactile properties. As is inherent to our replication approach, in terms of hardness and hairiness, participants' assessments showed significant differences to occur. However, in terms of stickiness and isotropy, most replicas maintained their tactile properties, as no significant differences could be found for respectively 14 and 13 pairs. For scratchiness, 10 samples were close to the original, while in terms of roughness, bumpiness, and uniformity, only 6 pairs did not show any significant deviations. In terms of tactile properties, the pairs of T-R$_{1\text{-casino}}$, T-R$_{10\text{-trend}}$, T-R$_{11\text{-onyx}}$ were not significantly different for a total of 6 metrics, while T-R$_{7\text{-cosy}}$, T-R$_{12\text{-cosmopolitan}}$, T-R$_{13\text{-easycare}}$, and T-R$_{15\text{-vintage}}$ for 5; T-R$_{5\text{-deluxe}}$ for 4, T-R$_{4\text{-havanna}}$ and T-R$_{14\text{-matrix}}$ for 3, T-R$_{3\text{-crown}}$, T-R$_{6\text{-clash}}$, and T-R$_{8\text{-florida}}$ and T-R$_{9\text{-yelda}}$ for only 2. The composition of T$_{2\text{-velvet}}$ proved it to be the most challenging surface sample to reproduce. Here, participants indicated to be able to quickly identify T$_{2\text{-velvet}}$ as the tactile perception of velvet was a unique sensation compared to all other samples.

Additionally, we found tactile perceptions to show high correlations with each other. Most importantly, the effect of increasing hardness was positively coupled to other properties, such as roughness, or bumpiness. From this, we see that the loss of hardness in our replication method influenced other tactile properties, as our manufacturing process only reproduced a surface's stable geometry. Intuitively seen, a hard surface makes the specific geometrical surface features more pronounced as they comply less to touch. This interaction may lead to increased subjective ratings of other perceptions. While hairiness did negatively correlate to hardness, its effect on other tactile assessments seemed to be limited. Here, we note that the influence of highly deformable structures, i.e., hairs, is minimized upon direct touch.

Does surface geometry replication convey the feeling of the original material? The high degree with which participants reported the original samples' material as *fabric-like* indicates that they correctly identified their material properties. Interestingly, in contrast to
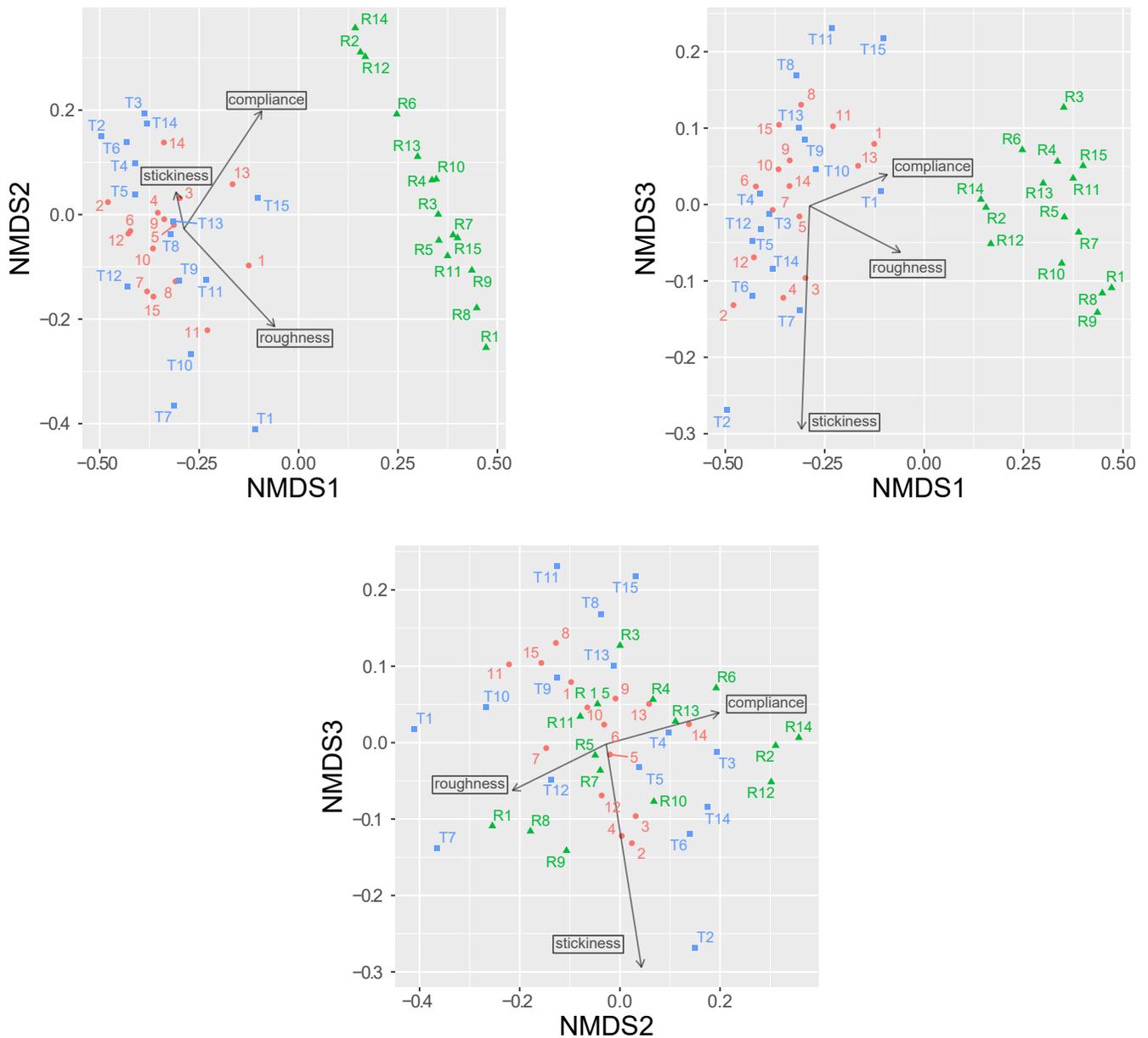
Figure 9: NMDS Perceptual space. Here, the distances between the original set of samples (blue), their physical measurements (red) and the replicated set (green) are visualized. The vectors represent the transformed axes of the physical measurement space taken from the original set of samples.

the original materials, our replicas manifest a wide variation in identified materials. Our set of reconstructed samples was printed using the same plastic material. We see that by changing the surface structure, participants indicated to perceive different materials. This underlines the influence of surface microgeometry on the perception of materials and its benefit to fabrication processes. Here, an opportunity exists to explore different methods to guide the

participant's perception towards a specific material, e.g., through visual priming in a Virtual Reality context.

Does surface geometry replication support a wide gamut of feel aesthetics? Our perceptual space allows us to inspect how the replication process influences the distance between the original and fabricated samples, see Figure 9. We can observe a clear separation between original materials and our replicas based on the perceived

hardness which is an effect of the manufacturing process that does not use elastic materials. However, the space occupied by the set of replicas shows the great variety with which microgeometry replication influenced the tactile impressions.

The similarity analysis results indicate that the replication process significantly affected the original and replicated samples' perceived distance. However, the distance created by the fabrication process did not seem to vary between different textures. From this, we can conclude that the replication process uniformly distorted perception between original and replicated samples, meaning no randomness was introduced in the process. Therefore, optimizing the replication process would optimize the haptic perception distance between the original and replicated sample.

Further visual analysis of the perceptual space in terms of roughness and stickiness vectors allows us to comprehend the surface replication distortion. Here, we observe that the shift between original and reproduction potentially leads to perceptually good matches for certain other sample combinations, e.g, T-R$_{3\text{-crown}}$ with T$_{1\text{-casino}}$, T-R$_{2\text{-velvet}}$ with T$_{7\text{-cosy}}$, T-R$_{6\text{-clash}}$ with T$_{10\text{-trend}}$, and T-R$_{14\text{-matrix}}$ with T$_{12\text{-cosmopolitan}}$. These results indicate that a potential transformation function of haptic surface appropriation could guide the understanding of tactile properties before fabrication. Such a function can be integrated into existing literature, such as in [80], where authors present a tool for designing the *feel* aesthetics of objects to be fabricated.

6.2 Applications for Fabricating Haptics

Designing haptic experiences remains a challenging task. Our work is motivated by the lack of prototyping methods for haptic design [61], and the importance of supporting personalization by end-users [64]. Rather than relying on computational tools, surface capturing methods support both end-users and professionals to design their own *feel* aesthetics [80] guided by real-life tactile experiences. With our approach, designers could use portable capturing devices as illustrated in [42], to record information in the world around them and build custom tactile libraries. Using these, digital objects fabrication can be enriched with tactile properties using common modelling tools.

The results of our study show that stable surface replication supports the fabrication of materials with similar haptic properties to the originals. Our approach to capturing only the stable features corresponds well with how our participants perceived the presented materials. We found that the deformable hair-like features of the materials affect the perceived compliance but do not have an influence on the perceived geometrical attributes like roughness, bumpiness, and scratchiness. As a result, deformable hair-like structures can be integrated into compliance and do not need to be present on the surface of the object. Focusing reproduction effort on stable features not only significantly facilitates the reproduction process but also increases the durability of reproduced surfaces as thin deformable features are most likely to be affected by mechanical wear.

Another exciting result of our study is the discovered coupling between the perceived properties. Prior works generally considered the perceived compliance, roughness, and stickiness as independent orthogonal directions [27, 78]. However, our results suggest that the increase in hardness caused the shift in perceived roughness of the 3D printed stimuli. We can distill this observation into a simple design rule. To successfully reproduce the perceived roughness, the designer should decrease the roughness of the object proportionally with the increase in hardness.

The printing process used in our work had a significant effect on the perceived haptic properties of our samples. Upon closer investigation, we observe that the pairwise dissimilarity captured by the original materials is still present in our digital replicas. This suggests that our manufacturing process applies a systematic transformation that effects the haptics of our digital replicas. This is further supported by the anecdotal assessment where participants were able to correctly identify the material of the original cloth samples but perceived a far wider gamut of materials in the digital replicas ranging from plastics, through stone, to wood. These results underline an uncertainty present in the material perception of the replicas, which could be guided through the addition of multisensory perception. As visual and haptic perception are statistically integrated [21], our approach could serve material perception using passive haptics in immersive virtual environments.

7 LIMITATIONS AND FUTURE WORK

While this paper presents a method for appropriating the haptic feedback of real-life textures for fabrication, there are several areas that should be investigated before such tools can become standardized in production pipelines.

Surface Texture Dataset. For analyzing the effects of the manufacturing process on the printed replicas we needed a representative dataset of samples that vary in compliance, geometrical features, and used materials. We opted for a set of 15 cloth samples that we show achieve good coverage in both measured and perceived assessments with the hopes that the results we achieve here would generalize to other material categories. An interesting direction of future work is to investigate new materials, e.g., leathers, metals, or woods, and observe if the results from this work generalize beyond our cloth samples.

Extending the Haptic Gamut. The individual material perceptions revealed that our manufacturing device can produce materials with a wide range of perceived qualities ranging from plastic-like to wood-like. A potential future work lies in further exploring the classes of materials that can be manufactured and quantifying the haptic gamut of a particular manufacturing device.

Based on observations from the psychophysical experiment, we suggest that reproducing the stable geometry is sufficient for matching the perceived roughness in many cases and that any small deformable features on the surface can be interpreted as compliance. However, to manufacture perfect replicas thin hair-like structures would need to be reproduced as they are perceivable based on the interaction mode. To this aim, the results of existing work could easily be leveraged [18, 47]. An interesting future work lies in evaluating how important the hair-like structures are to material perception and if the perception and affordance of material is significantly affected by leaving them out.

Tactile Matching. During the individual assessment analysis, we found a surprising result that reproducing the surface geometry

is not always sufficient to match the perceived roughness. We explained this by an effect on the compliance of the sample on the perception of roughness. It is possible that such coupled effects also affect the perception of other physical attributes like hardness and friction. An interesting avenue for future work would be to investigate materials that match in a physical property but manifest extreme variation in others. This would allow us to investigate how we can leverage the perceptual coupling between individual physical parameters to design better haptic experiences.

Our digital replicas manifest similar perceived friction to the original materials. While we did not specifically optimize for the perceived friction our reproduction process relies on mimicking the surface geometry which is one of the governing factors for friction [69]. The second important factor is the used materials. An interesting direction of future work would be to investigate how much influence of perceived friction do common manufacturing materials have and how much we can affect the perceived friction by adjusting the surface geometry.

Printing Technology. Our results are dependent on a sufficient printing resolution to reproduce the surface microgeometry. Unfortunately, common consumer 3D-printing technologies utilize FDM approaches, which relies on filaments at scales that dominate the haptic feedback of many everyday materials. However, higher resolution printing techniques are slowly becoming more accessible. Resin printers with comparable resolution to multijet printers are becoming available at competitive prices to FDMs. We believe that now is the correct time to study the haptics achievable with higher resolution processes, as the results discovered today will help makers design haptic experiences soon.

Our study focused on the most commonly available material for printing, i.e., hard plastics. We believe our results are robust to specific plastic selection as the main difference will be in the coefficient of friction between the material and the finger. There seems to be only a weak correlation between friction and the remaining perceptual attributes. This indicates that changing the plastic material will likely not have a significant effect on other perceptual attributes. An exciting avenue for future work is to investigate the use of soft materials as the demonstrated coupling between hardness and roughness leads to an interesting optimization problem.

Future Strategies. The proposed observations and strategies for appropriating the haptics of real-life materials are valid only for the used fabrication process. Utilizing drastically different processes and/or materials would lead to perceivable differences in haptic response. While in principle our study design can be replicated for each new fabrication setup it might be inefficient in the number of samples and participants required. To this end, an interesting future work lies in identifying a minimal dataset that should be fabricated with a new process to calibrate the haptic reproduction capabilities.

8 CONCLUSION

In this work, we present an approach for adapting haptic experiences from real-life for manufacturing purposes. To this end, we implemented an existing pressure-based geometry acquisition process for recovering the stable microgeometry investigated during active touch. We use this method on a challenging set of 15 cloth samples that manifest a wide range of haptic properties. We evaluate the reproduction quality by conducting individual assessments of the perceived qualities. From our results, we see that that direct reproduction of a material's surface can approximate the perceived geometry of some materials but it is not sufficient to consistently mimic their haptics. However, both in terms of perceptual features, such as roughness, and material perceptions, our digital reproductions show a great variation only through alterations of their surface construction. Therefore, our fabrication process supports a wide gamut of *feel* aesthetics. Furthermore, we investigate the shift that occurs after replication and discover that the change in perception of the reproduced samples was not stochastic but rather followed a uniform transformation. To find this transformation we conduct a magnitude estimation study and recover a perceptual-space of our samples which we correlate with measurable physical attributes. We leverage our perceptual space to formulate direct strategies that can be applied to the digital designs to better resemble the haptic sensations of the original materials. We believe that the techniques proposed here will have direct benefits for fabrication methods of haptic features and that our findings can serve as a basis for the future development of the field. Our results provide insights for the field of haptic design by supporting hapticians in creating versatile haptic experiences through capturing real-world information for fabrication processes.

ACKNOWLEDGMENTS

REFERENCES

[1] Michelle Annett, Fraser Anderson, Walter Bischof, and Anoop Gupta. 2014. The pen is mightier: understanding stylus behaviour while inking on tablets. In *Proceedings of Graphics Interface 2014* (Montréal, Québec, Canada) *(GI 2014)*. Canadian Human-Computer Communications Society, Toronto, Ontario, Canada, 193–200.

[2] Olivier Bau, Ivan Poupyrev, Ali Israr, and Chris Harrison. 2010. TeslaTouch: Electrovibration for Touch Surfaces. In *Proceedings of the 23Nd Annual ACM Symposium on User Interface Software and Technology* (New York, New York, USA) *(UIST '10)*. ACM, New York, NY, USA, 283–292. https://doi.org/10.1145/1866029.1866074

[3] Wouter M. Bergmann Tiest. 2010. Tactual perception of material properties. *Vision Research* 50, 24 (2010), 2775 – 2782. https://doi.org/10.1016/j.visres.2010.10.005 Perception and Action: Part I.

[4] Wouter M. Bergmann Tiest and Astrid M.L. Kappers. 2006. Analysis of haptic perception of materials by multidimensional scaling and physical measurements of roughness and compressibility. *Acta Psychologica* 121, 1 (2006), 1 – 20. https://doi.org/10.1016/j.actpsy.2005.04.005

[5] Andrea Bianchi, Ian Oakley, Jong Keun Lee, Dong Soo Kwon, and Vassilis Kostakos. 2010. Haptics for Tangible Interaction: A Vibro-Tactile Prototype. In *Proceedings of the Fifth International Conference on Tangible, Embedded, and Embodied Interaction* (Funchal, Portugal) *(TEI '11)*. Association for Computing Machinery, New York, NY, USA, 283–284. https://doi.org/10.1145/1935701.1935764

[6] J Black. 2019. *DeGarmo's materials and processes in manufacturing.* Wiley, Hoboken.

[7] Grigore C. Burdea. 2000. Haptics issues in virtual environments. In *Proceedings Computer Graphics International 2000* (Geneva, Switzerland). IEEE Computer Society, 295–302. https://doi.org/10.1109/CGI.2000.852345

[8] Tom Carter, Sue Ann Seah, Benjamin Long, Bruce Drinkwater, and Sriram Subramanian. 2013. UltraHaptics: Multi-Point Mid-Air Haptic Feedback for Touch Surfaces. In *Proceedings of the 26th Annual ACM Symposium on User Interface Software and Technology* (St. Andrews, Scotland, United Kingdom)

(UIST '13). Association for Computing Machinery, New York, NY, USA, 505–514. https://doi.org/10.1145/2501988.2502018

[9] Xiaoujuan Chen, Fei Shao, Cathy Barnes, Tom Childs, and Brian Henson. 2009. Exploring Relationships between Touch Perception and Surface Physical Properties. *International Journal of Design* 3 (08 2009), 67–76.

[10] Youngjun Cho, Andrea Bianchi, Nicolai Marquardt, and Nadia Bianchi-Berthouze. 2016. RealPen: Providing Realism in Handwriting Tasks on Touch Surfaces Using Auditory-Tactile Feedback. In *Proceedings of the 29th Annual Symposium on User Interface Software and Technology* (Tokyo, Japan) *(UIST '16)*. ACM, New York, NY, USA, 195–205. https://doi.org/10.1145/2984511.2984550

[11] K. R. Clarke. 1993. Non-parametric multivariate analyses of changes in community structure. *Australian Journal of Ecology* 18, 1 (1993), 117–143. https://doi.org/10.1111/j.1442-9993.1993.tb00438.x

[12] Theresa Cooke, Sebastian Kannengiesser, Christian Wallraven, and Heinrich H. Bülthoff. 2006. Object Feature Validation Using Visual and Haptic Similarity Ratings. *ACM Trans. Appl. Percept.* 3, 3 (July 2006), 239–261. https://doi.org/10.1145/1166087.1166093

[13] Michael A Costa, Mark R Cutkosky, and Sonie Lau. 2000. Roughness perception of haptically displayed fractal surfaces. 69, 2 (2000), 1073–1079.

[14] Heather Culbertson and Katherine J. Kuchenbecker. 2017. Importance of Matching Physical Friction, Hardness, and Texture in Creating Realistic Haptic Virtual Surfaces. *IEEE Transactions on Haptics* 10, 1 (2017), 63–74. https://doi.org/10.1109/TOH.2016.2598751

[15] Heather Culbertson, Juliette Unwin, Benjamin E. Goodman, and Katherine J. Kuchenbecker. 2013. Generating haptic texture models from unconstrained tool-surface interactions. In *2013 World Haptics Conference (WHC)*. 295–300. https://doi.org/10.1109/WHC.2013.6548424

[16] Jérémy Danna and Jean-Luc Velay. 2015. Basic and supplementary sensory feedback in handwriting. *Frontiers in Psychology* 6 (2015), 169. https://doi.org/10.3389/fpsyg.2015.00169

[17] Donald Degraen, Anna Reindl, Akhmajon Makhsadov, André Zenner, and Antonio Krüger. 2020. Envisioning Haptic Design for Immersive Virtual Environments. In *Companion Publication of the 2020 ACM Designing Interactive Systems Conference* (Eindhoven, Netherlands) *(DIS' 20 Companion)*. Association for Computing Machinery, New York, NY, USA, 287–291. https://doi.org/10.1145/3393914.3395870

[18] Donald Degraen, André Zenner, and Antonio Krüger. 2019. Enhancing Texture Perception in Virtual Reality Using 3D-Printed Hair Structures. In *Proceedings of the 2019 CHI Conference on Human Factors in Computing Systems* (Glasgow, Scotland Uk) *(CHI '19)*. Association for Computing Machinery, New York, NY, USA, 1–12. https://doi.org/10.1145/3290605.3300479

[19] Ulas Yaman Melik Dolen and Christoph Hoffmann. 2017. Formation of Patterned Indentations for Additive Manufacturing Applications. (Jan. 2017). https://doi.org/10.5281/zenodo.1160300

[20] S. Dong, W. Yuan, and E. H. Adelson. 2017. Improved GelSight tactile sensor for measuring geometry and slip. *CoRR* abs/1708.00922 (2017), 137–144. http://arxiv.org/abs/1708.00922

[21] Marc O. Ernst and Martin S. Banks. 2002. Humans integrate visual and haptic information in a statistically optimal fashion. *Nature* 415, 6870 (Jan. 2002), 429–433. https://doi.org/10.1038/415429a

[22] Alberto Gallace and Charles Spence. 2014. *In touch with the future: The sense of touch from cognitive neuroscience to virtual reality*. OUP Oxford. https://doi.org/10.1093/acprof:oso/9780199644469.001.0001

[23] Daniel Groeger, Martin Feick, Anusha Withana, and Jürgen Steimle. 2019. Tactlets: Adding Tactile Feedback to 3D Objects Using Custom Printed Controls. In *Proceedings of the 32nd Annual ACM Symposium on User Interface Software and Technology* (New Orleans, LA, USA) *(UIST '19)*. Association for Computing Machinery, New York, NY, USA, 923–936. https://doi.org/10.1145/3332165.3347937

[24] Vijaya L. Guruswamy, Jochen Lang, and Won-Sook Lee. 2009. Modelling of haptic vibration textures with infinite-impulse-response filters. In *2009 IEEE International Workshop on Haptic Audio visual Environments and Games*. 105–110. https://doi.org/10.1109/HAVE.2009.5356133

[25] Vijaya Lakshmi Guruswamy, Jochen Lang, and Won-Sook Lee. 2011. IIR Filter Models of Haptic Vibration Textures. *IEEE Transactions on Instrumentation and Measurement* 60, 1 (Jan. 2011), 93–103. https://doi.org/10.1109/tim.2010.2065751

[26] Richard Helps and Clarissa Helps. 2016. Measuring Stylus and Tablet Performance for Usability in Sketching. In *Proceedings of the 5th Annual Conference on Research in Information Technology* (Boston, Massachusetts, USA) *(RIIT '16)*. Association for Computing Machinery, New York, NY, USA, 19–24. https://doi.org/10.1145/2978178.2978186

[27] Mark Hollins, Sliman Bensmaïa, Kristie Karlof, and Forrest Young. 2000. Individual differences in perceptual space for tactile textures: Evidence from multidimensional scaling. *Perception & Psychophysics* 62, 8 (01 Dec 2000), 1534–1544. https://doi.org/10.3758/BF03212154

[28] Mark Hollins, Richard Faldowski, Suman Rao, and Forrest Young. 1993. Perceptual dimensions of tactile surface texture: A multidimensional scaling analysis. *Perception & Psychophysics* 54, 6 (01 Nov 1993), 697–705. https://doi.org/10.3758/BF03211795

[29] Scott E. Hudson. 2014. Printing Teddy Bears: A Technique for 3D Printing of Soft Interactive Objects. In *Proceedings of the SIGCHI Conference on Human Factors in Computing Systems* (Toronto, Ontario, Canada) *(CHI '14)*. Association for Computing Machinery, New York, NY, USA, 459–468. https://doi.org/10.1145/2556288.2557338

[30] Yasushi Ikei, Kazufumi Wakamatsu, and Shuichi Fukuda. 1997. Vibratory tactile display of image-based textures. *IEEE Computer Graphics and Applications* 17, 6 (1997), 53–61. https://doi.org/10.1109/38.626970

[31] Alexandra Ion, Robert Kovacs, Oliver S. Schneider, Pedro Lopes, and Patrick Baudisch. 2018. Metamaterial Textures. In *Proceedings of the 2018 CHI Conference on Human Factors in Computing Systems*. Association for Computing Machinery, New York, NY, USA, 1–12. https://doi.org/10.1145/3173574.3173910

[32] Ali Israr, Hong Z. Tan, and Charlotte M. Reed. 2006. Frequency and amplitude discrimination along the kinesthetic-cutaneous continuum in the presence of masking stimuli. *The Journal of the Acoustical Society of America* 120, 5 (2006), 2789–2800. https://doi.org/10.1121/1.2354022

[33] Micah K. Johnson and Edward H. Adelson. 2009. Retrographic sensing for the measurement of surface texture and shape. In *2009 IEEE Conference on Computer Vision and Pattern Recognition*. 1070–1077. https://doi.org/10.1109/cvpr.2009.5206534

[34] Micah K. Johnson, Forrester Cole, Alvin Raj, and Edward H. Adelson. 2011. Microgeometry Capture Using an Elastomeric Sensor. *ACM Trans. Graph.* 30, 4, Article 46 (July 2011), 8 pages. https://doi.org/10.1145/2010324.1964941

[35] Erin Kim and Oliver Schneider. 2020. *Defining Haptic Experience: Foundations for Understanding, Communicating, and Evaluating HX*. Association for Computing Machinery, New York, NY, USA, 1–13. https://doi.org/10.1145/3313831.3376280

[36] Seung-Chan Kim, Ali Israr, and Ivan Poupyrev. 2013. Tactile Rendering of 3D Features on Touch Surfaces. In *Proceedings of the 26th Annual ACM Symposium on User Interface Software and Technology* (St. Andrews, Scotland, United Kingdom) *(UIST '13)*. ACM, New York, NY, USA, 531–538. https://doi.org/10.1145/2501988.2502020

[37] Stefan Klare and Angelika Peer. 2015. The Formable Object: A 24-Degree-of-Freedom Shape-Rendering Interface. *IEEE/ASME Transactions on Mechatronics* 20, 3 (June 2015), 1360–1371. https://doi.org/10.1109/tmech.2014.2341630

[38] Paul G. Kry and Dinesh K. Pai. 2006. Interaction Capture and Synthesis. *ACM Transactions on Graphics* 25, 3 (July 2006), 872–880. https://doi.org/10.1145/1141911.1141969

[39] Ron Kurtus. 2005. Determining the Coefficient of Friction.

[40] Gierad Laput, Xiang 'Anthony' Chen, and Chris Harrison. 2015. 3D Printed Hair: Fused Deposition Modeling of Soft Strands, Fibers, and Bristles. In *Proceedings of the 28th Annual ACM Symposium on User Interface Software & Technology* (Charlotte, NC, USA). ACM, New York, NY, USA, 593–597. https://doi.org/10.1145/2807442.2807484

[41] Minchen Li, Z Ac Hary Ferguson, Teseo Schneider, Timothy Langlois, Denis Zorin, Daniele Panozzo, Chenfanfu Jiang, and Danny M. Kaufman. 2020. Incremental Potential Contact: Intersection-and Inversion-Free, Large-Deformation Dynamics. *ACM Trans. Graph.* 39, 4, Article 49 (July 2020), 20 pages. https://doi.org/10.1145/3386569.3392425

[42] Rui Li, Robert Platt, Wenzhen Yuan, Andreas ten Pas, Nathan Roscup, Mandayam A. Srinivasan, and Edward Adelson. 2014. Localization and manipulation of small parts using GelSight tactile sensing. In *2014 IEEE/RSJ International Conference on Intelligent Robots and Systems*. 3988–3993. https://doi.org/10.1109/iros.2014.6943123

[43] Benjamin Long, Sue Ann Seah, Tom Carter, and Sriram Subramanian. 2014. Rendering Volumetric Haptic Shapes in Mid-Air Using Ultrasound. *ACM Transactions on Graphics* 33, 6, Article 181 (Nov. 2014), 10 pages. https://doi.org/10.1145/2661229.2661257

[44] Jonàs Martínez, Jérémie Dumas, and Sylvain Lefebvre. 2016. Procedural Voronoi Foams for Additive Manufacturing. *ACM Trans. Graph.* 35, 4, Article 44 (July 2016), 12 pages. https://doi.org/10.1145/2897824.2925922

[45] David J. Meyer, Michael A. Peshkin, and J. Edward Colgate. 2016. Tactile Paintbrush: A procedural method for generating spatial haptic texture. In *2016 IEEE Haptics Symposium (HAPTICS)*. 259–264. https://doi.org/10.1109/HAPTICS.2016.7463187

[46] Shogo Okamoto, Hikaru Nagano, and Yoji Yamada. 2013. Psychophysical Dimensions of Tactile Perception of Textures. *IEEE Transactions on Haptics* 6, 1 (2013), 81–93. https://doi.org/10.1109/toh.2012.32

[47] Jifei Ou, Gershon Dublon, Chin-Yi Cheng, Felix Heibeck, Karl Willis, and Hiroshi Ishii. 2016. Cilllia: 3D Printed Micro-Pillar Structures for Surface Texture, Actuation and Sensing. In *Proceedings of the 2016 CHI Conference on Human Factors in Computing Systems* (San Jose, California, USA) *(CHI '16)*. ACM, New York, NY, USA, 5753–5764. https://doi.org/10.1145/2858036.2858257

[48] Claudio Pacchierotti, Domenico Prattichizzo, and Katherine J. Kuchenbecker. 2016. Cutaneous Feedback of Fingertip Deformation and Vibration for Palpation in Robotic Surgery. *IEEE Transactions on Biomedical Engineering* 63, 2 (Feb 2016), 278–287. https://doi.org/10.1109/TBME.2015.2455932

[49] Dinesh K Pai and Peter Rizun. 2003. The WHaT: A wireless haptic texture sensor. In *11th Symposium on Haptic Interfaces for Virtual Environment and Teleoperator*

Systems, 2003. HAPTICS 2003. Proceedings. IEEE, 3–9. https://doi.org/10.1109/haptic.2003.1191210

[50] Julian Panetta, Qingnan Zhou, Luigi Malomo, Nico Pietroni, Paolo Cignoni, and Denis Zorin. 2015. Elastic Textures for Additive Fabrication. *ACM Trans. Graph.* 34, 4, Article 135 (July 2015), 12 pages. https://doi.org/10.1145/2766937

[51] Huaishu Peng, Jennifer Mankoff, Scott E. Hudson, and James McCann. 2015. A Layered Fabric 3D Printer for Soft Interactive Objects. In *Proceedings of the 33rd Annual ACM Conference on Human Factors in Computing Systems* (Seoul, Republic of Korea) *(CHI '15).* Association for Computing Machinery, New York, NY, USA, 1789–1798. https://doi.org/10.1145/2702123.2702327

[52] Alvaro G. Perez, Daniel Lobo, Francesco Chinello, Gabriel Cirio, Monica Malvezzi, Jose San Martin, Domenico Prattichizzo, and Miguel A. Otaduy. 2017. Optimization-Based Wearable Tactile Rendering. *IEEE Transactions on Haptics* 10, 2 (April 2017), 254–264. https://doi.org/10.1109/toh.2016.2619708

[53] Michal Piovarči, Danny M. Kaufman, David I. W. Levin, and Piotr Didyk. 2020. Fabrication-in-the-Loop Co-Optimization of Surfaces and Styli for Drawing Haptics. *ACM Trans. Graph.* 39, 4, Article 116 (July 2020), 16 pages. https://doi.org/10.1145/3386569.3392467

[54] Michal Piovarči, David I.W. Levin, Danny Kaufman, and Piotr Didyk. 2018. Perception-Aware Modeling and Fabrication of Digital Drawing Tools. *ACM Transactions on Graphics (Proc. SIGGRAPH)* 37, 4 (2018).

[55] Michal Piovarči, David I. W. Levin, Jason Rebello, Desai Chen, Roman Ďurikovič, Hanspeter Pfister, Wojciech Matusik, and Piotr Didyk. 2016. An Interaction-Aware, Perceptual Model for Non-Linear Elastic Objects. *ACM Trans. Graph.* 35, 4, Article 55 (July 2016), 13 pages. https://doi.org/10.1145/2897824.2925885

[56] Michael L. Rivera and Scott E. Hudson. 2019. Desktop Electrospinning: A Single Extruder 3D Printer for Producing Rigid Plastic and Electrospun Textiles. In *Proceedings of the 2019 CHI Conference on Human Factors in Computing Systems* (Glasgow, Scotland Uk) *(CHI '19).* Association for Computing Machinery, New York, NY, USA, 1–12. https://doi.org/10.1145/3290605.3300434

[57] Michael L. Rivera, Melissa Moukperian, Daniel Ashbrook, Jennifer Mankoff, and Scott E. Hudson. 2017. Stretching the Bounds of 3D Printing with Embedded Textiles. In *Proceedings of the 2017 CHI Conference on Human Factors in Computing Systems* (Denver, Colorado, USA) *(CHI '17).* Association for Computing Machinery, New York, NY, USA, 497–508. https://doi.org/10.1145/3025453.3025460

[58] Gabriel Robles-De-La-Torre. 2006. The importance of the sense of touch in virtual and real environments. *IEEE MultiMedia* 13, 3 (July 2006), 24–30. https://doi.org/10.1109/MMUL.2006.69

[59] Joseph M. Romano and Katherine J. Kuchenbecker. 2012. Creating Realistic Virtual Textures from Contact Acceleration Data. *IEEE Transactions on Haptics* 5, 2 (April 2012), 109–119. https://doi.org/10.1109/toh.2011.38

[60] Satoshi Saga and Ramesh Raskar. 2012. Feel through Window: Simultaneous Geometry and Texture Display Based on Lateral Force. In *SIGGRAPH Asia 2012 Emerging Technologies* (Singapore, Singapore) *(SA '12).* Association for Computing Machinery, New York, NY, USA, 1–3. https://doi.org/10.1145/2407707.2407715

[61] Oliver Schneider, Karon MacLean, Colin Swindells, and Kellogg Booth. 2017. Haptic experience design: What hapticians do and where they need help. *International Journal of Human-Computer Studies* 107 (2017), 5–21. https://doi.org/10.1016/j.ijhcs.2017.04.004

[62] Philipp Schoessler, Daniel Windham, Daniel Leithinger, Sean Follmer, and Hiroshi Ishii. 2015. Kinetic Blocks: Actuated Constructive Assembly for Interaction and Display. In *Proceedings of the 28th Annual ACM Symposium on User Interface Software & Technology* (Charlotte, NC, USA) *(UIST '15).* Association for Computing Machinery, New York, NY, USA, 341–349. https://doi.org/10.1145/2807442.2807453

[63] Christian Schumacher, Bernd Bickel, Jan Rys, Steve Marschner, Chiara Daraio, and Markus Gross. 2015. Microstructures to Control Elasticity in 3D Printing. *ACM Trans. Graph.* 34, 4, Article 136 (July 2015), 13 pages. https://doi.org/10.1145/2766926

[64] Hasti Seifi, Matthew Chun, Colin Gallacher, Oliver Schneider, and Karon E. MacLean. 2020. How Do Novice Hapticians Design? A Case Study in Creating Haptic Learning Environments. *IEEE Transactions on Haptics* 13, 4 (Oct. 2020), 791–805. https://doi.org/10.1109/toh.2020.2968903

[65] Kazuhiro Shimonomura. 2019. Tactile Image Sensors Employing Camera: A Review. *Sensors (Basel, Switzerland)* 19, 18 (12 Sep 2019), 3933. https://doi.org/10.3390/s19183933

[66] Sunghwan Shin and Seungmoon Choi. 2018. Geometry-based haptic texture modeling and rendering using photometric stereo. In *2018 IEEE Haptics Symposium (HAPTICS).* IEEE. https://doi.org/10.1109/haptics.2018.8357186

[67] Pitchaya Sitthi-Amorn, Javier E. Ramos, Yuwang Wangy, Joyce Kwan, Justin Lan, Wenshou Wang, and Wojciech Matusik. 2015. MultiFab: A Machine Vision Assisted Platform for Multi-Material 3D Printing. *ACM Trans. Graph.* 34, 4, Article 129 (July 2015), 11 pages. https://doi.org/10.1145/2766962

[68] Lisa Skedung, Martin Arvidsson, Jun Young Chung, Christopher M. Stafford, Birgitta Berglund, and Mark W. Rutland. 2013. Feeling Small: Exploring the Tactile Perception Limits. *Scientific Reports* 3, 1 (12 Sep 2013), 2617. https://doi.org/10.1038/srep02617

[69] Lisa Skedung, Kathryn L. Harris, Elizabeth S. Collier, and Mark W. Rutland. 2020. The finishing touches: the role of friction and roughness in haptic perception of surface coatings. *Experimental Brain Research* 238, 6 (01 Jun 2020), 1511–1524. https://doi.org/10.1007/s00221-020-05831-w

[70] Mandayam A. Srinivasan and Cagatay Basdogan. 1997. Haptics in virtual environments: Taxonomy, research status, and challenges. *Computers & Graphics* 21, 4 (1997), 393–404. https://doi.org/10.1016/S0097-8493(97)00030-7

[71] Matti Strese, Clemens Schuwerk, and Eckehard Steinbach. 2015. Surface classification using acceleration signals recorded during human freehand movement. In *2015 IEEE World Haptics Conference (WHC).* IEEE. https://doi.org/10.1109/whc.2015.7177716

[72] Ryo Suzuki, Koji Yatani, Mark D. Gross, and Tom Yeh. 2018. Tabby: Explorable Design for 3D Printing Textures. *Pacific Graphics Short Papers* (2018). https://doi.org/10.2312/PG.20181273

[73] Ryo Suzuki, Tom Yeh, Koji Yatani, and Mark D. Gross. 2017. Autocomplete Textures for 3D Printing. *CoRR* abs/1703.05700 (2017). arXiv:1703.05700 http://arxiv.org/abs/1703.05700

[74] Haruki Takahashi and Jeeeun Kim. 2019. 3D Printed Fabric: Techniques for Design and 3D Weaving Programmable Textiles. In *Proceedings of the 32nd Annual ACM Symposium on User Interface Software and Technology* (New Orleans, LA, USA) *(UIST '19).* Association for Computing Machinery, New York, NY, USA, 43–51. https://doi.org/10.1145/3332165.3347896

[75] Haruki Takahashi and Homei Miyashita. 2016. Thickness Control Technique for Printing Tactile Sheets with Fused Deposition Modeling. In *Proceedings of the 29th Annual Symposium on User Interface Software and Technology* (Tokyo, Japan) *(UIST '16 Adjunct).* Association for Computing Machinery, New York, NY, USA, 51–53. https://doi.org/10.1145/2984751.2985701

[76] Haruki Takahashi and Homei Miyashita. 2017. Expressive Fused Deposition Modeling by Controlling Extruder Height and Extrusion Amount. In *Proceedings of the 2017 CHI Conference on Human Factors in Computing Systems* (Denver, Colorado, USA) *(CHI '17).* Association for Computing Machinery, New York, NY, USA, 5065–5074. https://doi.org/10.1145/3025453.3025933

[77] Yuta Takeuchi, Sho Kamuro, Kouta Minamizawa, and Susumu Tachi. 2012. Haptic Duplicator. In *Proceedings of the 2012 Virtual Reality International Conference* (Laval, France) *(VRIC '12).* Association for Computing Machinery, New York, NY, USA, Article 30, 2 pages. https://doi.org/10.1145/2331714.2331749

[78] Wouter M. Bergmann Tiest and Astrid M.L. Kappers. 2006. Analysis of haptic perception of materials by multidimensional scaling and physical measurements of roughness and compressibility. *Acta Psychologica* 121, 1 (Jan. 2006), 1–20. https://doi.org/10.1016/j.actpsy.2005.04.005

[79] Wouter M. Bergmann Tiest and Astrid M. L. Kappers. 2009. Tactile perception of thermal diffusivity. *Attention, Perception, & Psychophysics* 71, 3 (April 2009), 481–489. https://doi.org/10.3758/app.71.3.481

[80] Cesar Torres, Tim Campbell, Neil Kumar, and Eric Paulos. 2015. HapticPrint: Designing Feel Aesthetics for Digital Fabrication. In *Proceedings of the 28th Annual ACM Symposium on User Interface Software & Technology* (Charlotte, NC, USA) *(UIST '15).* ACM, New York, NY, USA, 583–591. https://doi.org/10.1145/2807442.2807492

[81] Chelsea Tymms, Esther P. Gardner, and Denis Zorin. 2018. A Quantitative Perceptual Model for Tactile Roughness. *ACM Trans. Graph.* 37, 5, Article 168 (Oct. 2018), 14 pages. https://doi.org/10.1145/3186267

[82] Yasemin Vardar, Christian Wallraven, and Katherine J. Kuchenbecker. 2019. Fingertip Interaction Metrics Correlate with Visual and Haptic Perception of Real Surfaces. In *2019 IEEE World Haptics Conference (WHC).* IEEE. https://doi.org/10.1109/whc.2019.8816095

[83] Mickeal Verschoor, Dan Casas, and Miguel A. Otaduy. 2020. Tactile Rendering Based on Skin Stress Optimization. *ACM Trans. Graph.* 39, 4, Article 90 (July 2020), 13 pages. https://doi.org/10.1145/3386569.3392398

[84] Steven S Wall and William Seymour Harwin. 1999. Modelling of surface identifying characteristics using fourier series. (1999).

[85] Qi Wang and Vincent Hayward. 2008. Tactile Synthesis and Perceptual Inverse Problems Seen from the Viewpoint of Contact Mechanics. *ACM Transactions on Applied Perception* 5, 2, Article 7 (May 2008), 19 pages. https://doi.org/10.1145/1279920.1279921

[86] Kentaro Yasu. 2017. Magnetic Plotter: A Macrotexture Design Method Using Magnetic Rubber Sheets. In *Proceedings of the 2017 CHI Conference on Human Factors in Computing Systems* (Denver, Colorado, USA) *(CHI '17).* ACM, New York, NY, USA, 4983–4993. https://doi.org/10.1145/3025453.3025702

[87] Kentaro Yasu. 2019. Magnetact: Magnetic-Sheet-Based Haptic Interfaces for Touch Devices. In *Proceedings of the 2019 CHI Conference on Human Factors in Computing Systems* (Glasgow, Scotland Uk) *(CHI '19).* Association for Computing Machinery, New York, NY, USA, 1–8. https://doi.org/10.1145/3290605.3300470

[88] Kentaro Yasu. 2020. MagneLayer: Force Field Fabrication for Rapid Prototyping of Haptic Interactions. In *ACM SIGGRAPH 2020 Labs* (Virtual Event, USA) *(SIGGRAPH '20).* Association for Computing Machinery, New York, NY, USA, Article 4, 2 pages. https://doi.org/10.1145/3388763.3407761

[89] Kentaro Yasu and Yuichiro Katsumoto. 2015. Bump Ahead: Easy-to-Design Haptic Surface Using Magnet Array. In *SIGGRAPH Asia 2015 Emerging Technologies*

(Kobe, Japan) *(SA '15)*. Association for Computing Machinery, New York, NY, USA, Article 3, 3 pages. https://doi.org/10.1145/2818466.2818478

[90] Masaaki Yoshida. 1968. Dimensions of Tactual Impressions (1). *Japanese Psychological Research* 10, 3 (1968), 123–137. https://doi.org/10.4992/psycholres1954.10.123

[91] T. Yoshioka, S. J. Bensmaïa, J. C. Craig, and S. S. Hsiao. 2007. Texture perception through direct and indirect touch: An analysis of perceptual space for tactile textures in two modes of exploration. *Somatosensory & Motor Research* 24, 1-2 (2007), 53–70. https://doi.org/10.1080/08990220701318163

[92] Wenzhen Yuan, Rui Li, Mandayam A. Srinivasan, and Edward H. Adelson. 2015. Measurement of shear and slip with a GelSight tactile sensor. In *2015 IEEE International Conference on Robotics and Automation (ICRA)*. IEEE. https://doi.org/10.1109/icra.2015.7139016

[93] Wenzhen Yuan, Shaoxiong Wang, Siyuan Dong, and Edward Adelson. 2017. Connecting Look and Feel: Associating the visual and tactile properties of physical materials. arXiv:1704.03822 [cs.CV]

[94] Wenzhen Yuan, Chenzhuo Zhu, Andrew Owens, Mandayam A. Srinivasan, and Edward H. Adelson. 2017. Shape-independent Hardness Estimation Using Deep Learning and a GelSight Tactile Sensor. *CoRR* abs/1704.03955 (2017). http://arxiv.org/abs/1704.03955

[95] Ruo Zhang, Ping-Sing Tsai, J.E. Cryer, and M. Shah. 1999. Shape-from-shading: a survey. *IEEE Transactions on Pattern Analysis and Machine Intelligence* 21, 8 (1999), 690–706. https://doi.org/10.1109/34.784284

[96] Bo Zhu, Mélina Skouras, Desai Chen, and Wojciech Matusik. 2017. Two-Scale Topology Optimization with Microstructures. *ACM Trans. Graph.* 36, 4, Article 120b (July 2017), 16 pages. https://doi.org/10.1145/3072959.3095815

A INDIVIDUAL TACTILE RATINGS

Hardness (rows R1–R15, T1–T15 left) / Roughness (right)

	R1	R2	R3	R4	R5	R6	R7	R8	R9	R10	R11	R12	R13	R14	R15	T1	T2	T3	T4	T5	T6	T7	T8	T9	T10	T11	T12	T13	T14	T15
R1	R1	0.00	0.22	0.11	0.54	0.01	1.00	1.00	1.00	0.03	0.90	0.00	0.00	0.00	1.00	0.68	0.00	0.00	0.00	0.00	0.00	0.00	0.00	0.00	0.01	0.00	0.00	0.00	0.00	0.00
R2	1.00	R2	0.06	0.17	0.01	1.00	0.00	0.00	0.00	0.69	0.00	1.00	1.00	1.00	0.01	0.03	0.00	0.28	0.91	1.00	0.00	1.00	1.00	1.00	1.00	1.00	1.00	1.00	1.00	1.00
R3	1.00	1.00	R3	1.00	1.00	1.00	1.00	0.55	0.32	1.00	1.00	1.00	1.00	0.22	1.00	1.00	0.00	0.00	0.00	0.00	0.00	0.34	0.24	0.04	0.45	1.00	0.01	0.24	0.00	0.08
R4	1.00	1.00	1.00	R4	1.00	1.00	1.00	1.00	0.17	0.15	1.00	1.00	1.00	0.63	1.00	1.00	0.00	0.00	0.00	0.00	0.00	0.58	0.62	0.15	0.52	1.00	0.01	0.62	0.00	0.19
R5	1.00	1.00	1.00	1.00	R5	1.00	1.00	1.00	0.75	1.00	1.00	0.45	0.86	0.06	1.00	1.00	0.00	0.00	0.00	0.00	0.00	0.11	0.04	0.02	0.11	0.96	0.00	0.06	0.00	0.01
R6	1.00	1.00	1.00	1.00	1.00	R6	0.13	0.01	0.01	1.00	0.70	1.00	1.00	1.00	0.69	1.00	0.00	0.05	0.22	0.66	0.00	1.00	1.00	1.00	1.00	1.00	1.00	1.00	0.36	1.00
R7	1.00	1.00	1.00	1.00	1.00	1.00	R7	1.00	1.00	1.00	1.00	0.01	0.03	0.00	1.00	1.00	0.00	0.00	0.00	0.00	0.00	0.01	0.00	0.00	0.04	0.01	0.00	0.00	0.00	0.00
R8	1.00	1.00	1.00	1.00	1.00	1.00	1.00	R8	1.00	0.08	1.00	0.00	0.00	0.00	1.00	1.00	0.00	0.00	0.00	0.00	0.00	0.00	0.00	0.00	0.01	0.00	0.00	0.00	0.00	0.00
R9	1.00	1.00	1.00	1.00	1.00	1.00	0.72	1.00	R9	0.05	1.00	0.00	0.00	0.00	1.00	0.91	0.00	0.00	0.00	0.00	0.00	0.00	0.00	0.00	0.01	0.00	0.00	0.00	0.00	0.00
R10	1.00	1.00	1.00	1.00	1.00	1.00	1.00	1.00	1.00	R10	1.00	1.00	1.00	1.00	1.00	1.00	0.00	0.00	0.00	0.01	0.00	1.00	1.00	0.38	1.00	1.00	0.10	1.00	0.00	1.00
R11	1.00	1.00	1.00	1.00	1.00	1.00	1.00	1.00	1.00	1.00	R11	0.10	0.17	0.01	1.00	1.00	0.00	0.00	0.00	0.00	0.00	0.04	0.01	0.00	0.05	0.15	0.00	0.01	0.00	0.00
R12	1.00	1.00	1.00	1.00	1.00	1.00	1.00	1.00	0.51	1.00	1.00	R12	1.00	1.00	0.18	0.90	0.00	0.09	0.22	0.59	0.00	1.00	1.00	1.00	1.00	1.00	1.00	1.00	0.46	1.00
R13	1.00	1.00	1.00	1.00	1.00	1.00	1.00	1.00	1.00	1.00	1.00	1.00	R13	1.00	0.68	1.00	0.00	0.00	0.01	0.00	0.00	1.00	1.00	1.00	1.00	1.00	0.46	1.00	0.01	1.00
R14	1.00	1.00	0.44	1.00	1.00	1.00	1.00	1.00	1.00	0.06	1.00	1.00	1.00	R14	0.04	0.15	0.00	0.38	1.00	1.00	0.00	1.00	1.00	1.00	1.00	1.00	1.00	1.00	1.00	1.00
R15	1.00	1.00	1.00	1.00	1.00	1.00	1.00	1.00	1.00	1.00	1.00	1.00	1.00	1.00	R15	1.00	0.00	0.00	0.00	0.00	0.00	0.11	0.05	0.01	0.23	0.49	0.00	0.05	0.00	0.02
T1	0.00	0.04	0.00	0.02	0.00	0.01	0.00	0.00	0.00	0.00	0.00	0.00	0.00	0.08	0.01	T1	0.00	0.00	0.00	0.00	0.00	0.19	0.13	0.03	0.17	1.00	0.00	0.14	0.00	0.04
T2	0.00	0.00	0.00	0.00	0.00	0.00	0.00	0.00	0.00	0.00	0.00	0.00	0.00	0.00	0.00	0.00	T2	0.04	0.01	0.03	1.00	0.00	0.00	0.00	0.00	0.00	0.00	0.00	0.00	0.00
T3	0.00	0.00	0.00	0.00	0.00	0.00	0.00	0.00	0.00	0.00	0.00	0.00	0.00	0.00	0.00	1.00	0.04	T3	1.00	1.00	1.00	0.72	0.02	1.00	0.16	0.00	1.00	0.09	1.00	0.17
T4	0.00	0.00	0.00	0.00	0.00	0.00	0.00	0.00	0.00	0.00	0.00	0.00	0.00	0.00	0.00	0.03	0.18	1.00	T4	1.00	1.00	1.00	0.03	1.00	0.55	0.00	1.00	0.24	1.00	0.29
T5	0.00	0.00	0.00	0.00	0.00	0.00	0.00	0.00	0.00	0.00	0.00	0.00	0.00	0.00	0.00	0.00	1.00	1.00	1.00	T5	1.00	1.00	0.18	1.00	1.00	0.01	1.00	0.80	1.00	0.99
T6	0.00	0.00	0.00	0.00	0.00	0.00	0.00	0.00	0.00	0.00	0.00	0.00	0.00	0.00	0.00	0.94	1.00	1.00	1.00	1.00	T6	0.01	0.00	0.05	0.00	0.00	0.03	0.00	0.38	0.00
T7	0.00	0.00	0.00	0.00	0.00	0.00	0.00	0.00	0.00	0.00	0.00	0.00	0.00	0.00	0.00	0.00	1.00	1.00	1.00	1.00	1.00	T7	1.00	1.00	1.00	1.00	1.00	1.00	1.00	1.00
T8	0.00	0.01	0.00	0.01	0.00	0.00	0.00	0.00	0.00	0.00	0.00	0.00	0.00	0.02	0.00	1.00	0.00	1.00	1.00	0.09	0.28	0.18	T8	1.00	1.00	1.00	1.00	1.00	0.11	1.00
T9	0.00	0.02	0.00	0.02	0.00	0.01	0.00	0.00	0.00	0.01	0.00	0.05	0.00	1.00	0.00	1.00	0.00	1.00	1.00	0.20	0.40	0.34	1.00	T9	1.00	1.00	1.00	1.00	1.00	1.00
T10	0.00	0.00	0.00	0.00	0.00	0.00	0.00	0.00	0.00	0.00	0.00	0.00	0.00	0.00	0.00	0.32	0.03	1.00	1.00	1.00	1.00	1.00	1.00	1.00	T10	1.00	1.00	1.00	1.00	1.00
T11	0.00	0.01	0.00	0.01	0.00	0.00	0.00	0.00	0.00	0.00	0.00	0.00	0.00	0.02	0.00	1.00	0.00	1.00	1.00	0.04	0.13	0.09	1.00	1.00	1.00	T11	0.22	1.00	0.00	1.00
T12	0.00	0.00	0.00	0.00	0.00	0.00	0.00	0.00	0.00	0.00	0.00	0.00	0.00	0.00	0.00	0.00	1.00	1.00	1.00	1.00	1.00	1.00	0.09	0.16	1.00	0.04	T12	1.00	1.00	1.00
T13	0.00	0.00	0.00	0.00	0.00	0.00	0.00	0.00	0.00	0.00	0.00	0.00	0.00	0.00	0.00	1.00	0.00	1.00	1.00	0.09	0.26	0.18	1.00	1.00	1.00	1.00	0.08	T13	0.58	1.00
T14	0.00	0.00	0.00	0.00	0.00	0.00	0.00	0.00	0.00	0.00	0.00	0.00	0.00	0.00	0.00	1.00	0.00	1.00	1.00	0.44	1.00	0.76	1.00	1.00	1.00	1.00	0.45	1.00	T14	0.72
T15	0.03	0.93	0.01	0.93	0.33	0.34	0.23	0.03	0.00	0.04	0.08	0.72	0.38	1.00	0.19	1.00	0.00	1.00	0.13	0.01	0.03	0.02	1.00	0.00	0.64	1.00	0.01	1.00	1.00	T15

Figure 10: P-values (green, < 0.05; blue, >= 0.05) of the Wilcoxon signed ranks tests (Bonferroni-Holm correction) for all comparisons for hardness (left) and roughness (right). The ratings of hardness and roughness were found to significantly differ depending on the sample (hardness, $\chi^2(29) = 445.83$, $p < .001$; roughness, $\chi^2(29) = 382.29$, $p < .001$).

Bumpiness (left) / Stickiness (right)

	R1	R2	R3	R4	R5	R6	R7	R8	R9	R10	R11	R12	R13	R14	R15	T1	T2	T3	T4	T5	T6	T7	T8	T9	T10	T11	T12	T13	T14	T15
R1	R1	1.00	1.00	1.00	1.00	1.00	1.00	1.00	1.00	1.00	1.00	1.00	1.00	1.00	1.00	1.00	0.03	0.32	1.00	1.00	0.08	1.00	1.00	1.00	1.00	1.00	1.00	1.00	1.00	1.00
R2	0.02	R2	1.00	1.00	1.00	1.00	1.00	1.00	1.00	1.00	1.00	1.00	1.00	1.00	1.00	1.00	0.02	0.54	1.00	1.00	0.09	1.00	1.00	1.00	1.00	0.23	1.00	0.17	1.00	1.00
R3	0.81	1.00	R3	1.00	1.00	1.00	1.00	1.00	1.00	1.00	1.00	1.00	1.00	1.00	1.00	1.00	0.01	0.08	1.00	0.94	0.02	1.00	0.61	1.00	1.00	1.00	1.00	0.40	0.94
R4	0.25	1.00	1.00	R4	1.00	1.00	1.00	1.00	1.00	1.00	1.00	1.00	1.00	1.00	1.00	1.00	0.02	0.16	1.00	1.00	0.06	1.00	1.00	1.00	1.00	1.00	1.00	1.00	0.88	1.00
R5	0.65	1.00	1.00	1.00	R5	1.00	1.00	1.00	1.00	1.00	1.00	1.00	1.00	1.00	1.00	1.00	0.01	0.12	1.00	1.00	0.03	1.00	0.98	1.00	1.00	1.00	1.00	1.00	0.71	1.00
R6	0.00	1.00	0.82	1.00	1.00	R6	1.00	1.00	1.00	1.00	1.00	1.00	1.00	1.00	1.00	1.00	0.08	1.00	1.00	1.00	0.43	1.00	1.00	1.00	1.00	1.00	1.00	1.00	1.00	1.00
R7	1.00	0.43	1.00	1.00	1.00	0.03	R7	1.00	1.00	1.00	1.00	1.00	1.00	1.00	1.00	1.00	0.01	0.11	1.00	1.00	0.03	1.00	0.77	1.00	1.00	1.00	1.00	1.00	0.57	1.00
R8	1.00	1.00	1.00	1.00	1.00	0.32	1.00	R8	1.00	1.00	1.00	1.00	1.00	1.00	1.00	1.00	0.02	0.20	1.00	0.92	0.05	1.00	0.81	0.99	1.00	1.00	1.00	1.00	0.72	0.77
R9	1.00	1.00	0.20	1.00	1.00	0.01	1.00	1.00	R9	1.00	1.00	1.00	1.00	1.00	1.00	1.00	0.07	0.50	1.00	1.00	0.13	1.00	1.00	1.00	1.00	1.00	1.00	1.00	1.00	1.00
R10	0.02	1.00	1.00	1.00	1.00	1.00	0.20	1.00	0.08	R10	1.00	1.00	1.00	1.00	1.00	1.00	0.03	0.73	1.00	1.00	0.10	1.00	1.00	1.00	1.00	1.00	1.00	1.00	1.00	1.00
R11	0.34	1.00	1.00	1.00	1.00	1.00	1.00	1.00	1.00	1.00	R11	1.00	1.00	1.00	1.00	1.00	0.03	0.36	1.00	1.00	0.10	1.00	1.00	1.00	1.00	1.00	1.00	1.00	1.00	1.00
R12	0.00	1.00	0.01	0.06	0.07	1.00	0.00	0.03	0.00	0.63	1.00	R12	1.00	1.00	1.00	1.00	0.41	1.00	1.00	1.00	1.00	1.00	1.00	1.00	1.00	1.00	1.00	1.00	1.00	1.00
R13	0.01	1.00	1.00	1.00	1.00	1.00	0.04	0.51	0.01	1.00	1.00	1.00	R13	1.00	1.00	1.00	0.31	1.00	1.00	1.00	0.54	1.00	1.00	1.00	1.00	1.00	1.00	1.00	1.00	1.00
R14	0.03	1.00	1.00	1.00	1.00	1.00	0.28	1.00	0.15	1.00	1.00	1.00	1.00	R14	1.00	1.00	0.07	1.00	1.00	1.00	0.34	1.00	1.00	1.00	1.00	1.00	1.00	1.00	1.00	1.00
R15	0.22	1.00	1.00	1.00	1.00	1.00	1.00	1.00	1.00	1.00	1.00	0.07	1.00	1.00	R15	1.00	0.00	0.03	0.54	0.28	0.01	1.00	0.16	0.30	0.59	1.00	0.50	1.00	0.11	0.27
T1	1.00	1.00	1.00	1.00	1.00	1.00	0.39	1.00	1.00	1.00	1.00	0.01	0.55	1.00	1.00	T1	0.05	1.00	1.00	0.32	1.00	1.00	1.00	1.00	1.00	1.00	1.00	1.00	1.00	1.00
T2	0.00	0.00	0.00	0.00	0.00	0.00	0.00	0.00	0.00	0.00	0.00	0.00	0.00	0.00	0.00	0.00	T2	1.00	1.00	1.00	1.00	0.16	1.00	1.00	0.23	1.00	0.17	1.00	1.00	1.00
T3	0.00	0.00	0.00	0.00	0.00	0.00	0.00	0.00	0.00	0.00	0.00	0.00	0.00	0.00	0.00	0.00	1.00	T3	1.00	1.00	1.00	1.00	1.00	1.00	1.00	1.00	1.00	1.00	1.00	1.00
T4	0.00	0.00	0.00	0.00	0.00	0.03	0.00	0.00	0.00	0.00	0.00	0.10	0.00	0.08	0.00	0.34	1.00	1.00	T4	1.00	1.00	1.00	1.00	1.00	1.00	1.00	1.00	1.00	1.00	1.00
T5	0.00	0.00	0.00	0.00	0.00	0.01	0.00	0.00	0.00	0.03	0.00	0.04	0.00	0.00	0.00	0.00	0.33	1.00	1.00	T5	1.00	1.00	1.00	1.00	1.00	1.00	1.00	1.00	1.00	1.00
T6	0.00	0.00	0.00	0.00	0.00	0.00	0.00	0.00	0.00	0.00	0.00	0.00	0.00	0.00	0.00	0.00	1.00	1.00	1.00	1.00	T6	1.00	1.00	1.00	0.90	1.00	1.00	1.00	1.00	1.00
T7	0.03	1.00	1.00	1.00	1.00	1.00	0.21	1.00	0.10	1.00	1.00	1.00	1.00	1.00	1.00	1.00	0.00	0.00	0.02	0.01	0.00	T7	0.57	1.00	1.00	1.00	1.00	1.00	1.00	1.00
T8	1.00	0.19	0.00	0.00	0.00	1.00	0.00	0.01	0.00	0.01	0.03	1.00	0.11	0.00	0.01	1.00	0.06	1.00	1.00	0.09	0.01	0.57	T8	1.00	1.00	1.00	1.00	1.00	0.72	0.77
T9	0.00	1.00	0.01	0.05	0.04	1.00	0.00	0.02	0.00	0.27	0.48	1.00	1.00	1.00	0.06	0.01	0.00	0.03	1.00	1.00	0.01	1.00	1.00	T9	1.00	1.00	1.00	1.00	1.00	1.00
T10	0.00	1.00	0.26	0.80	0.98	1.00	0.00	0.09	0.00	1.00	1.00	1.00	1.00	1.00	0.72	0.09	0.00	0.00	0.06	0.02	0.00	1.00	1.00	1.00	T10	1.00	1.00	1.00	1.00	1.00
T11	0.00	1.00	0.01	0.04	0.06	1.00	0.00	0.03	0.00	0.43	1.00	1.00	1.00	1.00	0.06	0.01	0.00	0.16	0.05	1.00	1.00	1.00	1.00	1.00	1.00	T11	1.00	1.00	1.00	1.00
T12	0.00	0.07	0.00	0.00	0.00	0.58	0.00	0.00	0.00	0.00	0.01	1.00	0.03	1.00	0.00	0.00	0.00	0.23	1.00	1.00	0.06	0.20	1.00	1.00	0.56	1.00	T12	1.00	1.00	1.00
T13	0.00	1.00	0.01	0.01	0.00	0.01	0.00	0.01	0.00	0.07	0.17	1.00	1.00	1.00	0.01	0.00	0.01	0.68	1.00	1.00	0.34	1.00	1.00	1.00	1.00	1.00	1.00	T13	1.00	1.00
T14	0.00	0.00	0.00	0.00	0.00	0.00	0.00	0.00	0.00	0.00	0.00	0.01	0.00	0.01	0.00	0.00	1.00	1.00	1.00	1.00	1.00	0.00	0.54	0.21	0.01	0.01	1.00	1.00	T14	1.00
T15	0.00	0.20	0.00	0.00	0.00	1.00	0.00	0.00	0.00	0.01	0.04	1.00	0.13	1.00	0.00	0.00	0.00	0.31	1.00	1.00	0.10	0.54	1.00	1.00	1.00	1.00	1.00	1.00	1.00	T15

Figure 11: P-values (green, < 0.05; blue, >= 0.05) of the Wilcoxon signed ranks tests (Bonferroni-Holm correction) for all comparisons for bumpiness (left) and stickiness (right). The ratings of bumpiness and stickiness were found to significantly differ depending on the sample (bumpiness, $\chi^2(29) = 393.01$, $p < .001$; stickiness, $\chi^2(29) = 172.08$, $p < .001$).

Figure 12 — Scratchiness (left) / Hairiness (right)

	R1	R2	R3	R4	R5	R6	R7	R8	R9	R10	R11	R12	R13	R14	R15	T1	T2	T3	T4	T5	T6	T7	T8	T9	T10	T11	T12	T13	T14	T15
R1	R1	1.00	1.00	1.00	1.00	1.00	1.00	1.00	1.00	1.00	1.00	1.00	1.00	1.00	1.00	0.00	0.01	0.09	0.00	0.00	0.17	0.00	0.00	0.00	0.00	0.00	0.00	0.00	0.01	0.15
R2	0.00	R2	1.00	1.00	1.00	1.00	1.00	1.00	1.00	1.00	1.00	1.00	1.00	1.00	1.00	0.00	0.03	0.20	0.00	0.01	0.32	0.00	0.00	0.00	0.00	0.00	0.00	0.00	0.02	0.32
R3	1.00	0.06	R3	1.00	1.00	1.00	1.00	1.00	1.00	1.00	1.00	1.00	1.00	1.00	1.00	0.00	0.01	0.03	0.00	0.00	0.05	0.00	0.00	0.00	0.00	0.00	0.00	0.00	0.00	0.04
R4	0.15	0.15	1.00	R4	1.00	1.00	1.00	1.00	1.00	1.00	1.00	1.00	1.00	1.00	1.00	0.00	0.03	0.26	0.01	0.01	0.46	0.00	0.00	0.00	0.00	0.00	0.00	0.00	0.03	0.56
R5	1.00	0.05	1.00	1.00	R5	1.00	1.00	1.00	1.00	1.00	1.00	1.00	1.00	1.00	1.00	0.00	0.00	0.03	0.00	0.00	0.05	0.00	0.00	0.00	0.00	0.00	0.00	0.00	0.00	0.03
R6	0.01	1.00	0.89	1.00	1.00	R6	1.00	1.00	1.00	1.00	1.00	1.00	1.00	1.00	1.00	0.00	0.01	0.08	0.00	0.00	0.14	0.00	0.00	0.00	0.00	0.00	0.00	0.00	0.01	0.11
R7	1.00	0.03	1.00	1.00	1.00	0.34	R7	1.00	1.00	1.00	1.00	1.00	1.00	1.00	1.00	0.00	0.01	0.06	0.00	0.00	0.10	0.00	0.00	0.00	0.00	0.00	0.00	0.00	0.00	0.07
R8	1.00	0.00	1.00	0.64	1.00	0.01	1.00	R8	1.00	1.00	1.00	1.00	1.00	1.00	1.00	0.00	0.03	0.26	0.00	0.01	0.58	0.00	0.00	0.00	0.00	0.00	0.00	0.00	0.02	0.49
R9	1.00	0.00	1.00	0.07	0.94	0.00	1.00	1.00	R9	1.00	1.00	1.00	1.00	1.00	1.00	0.00	0.01	0.09	0.00	0.00	0.20	0.00	0.00	0.00	0.00	0.00	0.00	0.00	0.01	0.18
R10	1.00	0.13	1.00	1.00	1.00	1.00	1.00	1.00	1.00	R10	1.00	1.00	1.00	1.00	1.00	0.00	0.01	0.05	0.00	0.00	0.10	0.00	0.00	0.00	0.00	0.00	0.00	0.00	0.00	0.07
R11	1.00	1.00	1.00	1.00	1.00	0.11	1.00	1.00	1.00	1.00	R11	1.00	1.00	1.00	1.00	0.00	0.01	0.08	0.00	0.00	0.16	0.00	0.00	0.00	0.00	0.00	0.00	0.00	0.00	0.13
R12	0.02	1.00	1.00	1.00	1.00	1.00	1.00	0.06	0.02	1.00	0.32	R12	1.00	1.00	1.00	0.00	0.02	0.16	0.00	0.01	0.26	0.00	0.00	0.00	0.00	0.00	0.00	0.00	0.01	0.24
R13	0.19	1.00	1.00	1.00	1.00	1.00	1.00	0.87	0.11	1.00	1.00	1.00	R13	1.00	1.00	0.00	0.02	0.14	0.00	0.00	0.30	0.00	0.00	0.00	0.00	0.00	0.00	0.00	0.01	0.25
R14	0.00	1.00	0.09	0.27	0.09	1.00	0.04	0.00	0.00	0.16	0.01	1.00	1.00	R14	1.00	0.00	0.08	0.75	0.02	0.04	1.00	0.00	0.00	0.00	0.00	0.00	0.00	0.01	0.08	1.00
R15	1.00	0.14	1.00	1.00	1.00	1.00	1.00	1.00	1.00	1.00	1.00	1.00	0.19	1.00	R15	0.00	0.01	0.05	0.00	0.00	0.10	0.00	0.00	0.00	0.00	0.00	0.00	0.00	0.00	0.07
T1	0.23	0.01	1.00	1.00	1.00	0.29	1.00	1.00	0.09	1.00	1.00	1.00	0.00	0.01		T1	1.00	0.15	1.00	0.98	1.00	1.00	1.00	1.00	1.00	1.00	1.00	1.00	1.00	0.10
T2	0.03	1.00	0.00	0.00	0.00	0.00	0.00	0.00	0.00	0.00	0.01	0.00	0.04	0.00		1.00	T2	1.00	1.00	1.00	1.00	1.00	1.00	1.00	1.00	1.00	1.00	1.00	1.00
T3	0.00	1.00	0.01	0.01	0.01	1.00	0.00	0.00	0.00	0.01	0.00	1.00	0.57	1.00	0.02	0.00	1.00	T3	1.00	1.00	1.00	0.00	0.67	1.00	0.15	1.00	0.05	1.00	1.00	1.00
T4	0.00	1.00	0.02	0.03	0.02	1.00	0.01	0.00	0.00	0.02	0.00	1.00	1.00	0.06		0.00	1.00	1.00	T4	1.00	1.00	0.02	1.00	1.00	1.00	1.00	0.45	1.00	1.00	1.00
T5	0.00	1.00	0.13	0.41	0.15	1.00	0.06	0.00	0.00	0.16	0.02	1.00	1.00	1.00	0.22	0.05	0.95	1.00	1.00	T5	1.00	0.02	1.00	1.00	1.00	1.00	0.30	1.00	1.00	1.00
T6	0.00	0.56	0.00	0.00	0.00	0.07	0.00	0.00	0.00	0.00	0.00	0.08	0.04	0.65	0.00	0.00	1.00	1.00	1.00	1.00	T6	0.03	1.00	1.00	1.00	1.00	0.27	1.00	1.00	1.00
T7	0.02	1.00	1.00	1.00	1.00	1.00	0.72	0.06	0.01	1.00	0.39	1.00	1.00	1.00	1.00	1.00	0.15	1.00	1.00	1.00	1.00	T7	1.00	0.33	1.00	0.02	1.00	0.09	0.04	0.00
T8	0.01	1.00	1.00	1.00	1.00	1.00	1.00	0.02	0.01	1.00	0.19	1.00	1.00	1.00	1.00	1.00	0.00	0.15	0.17	1.00	0.00	1.00	T8	1.00	1.00	1.00	1.00	1.00	1.00	0.27
T9	0.06	1.00	1.00	1.00	1.00	1.00	1.00	0.27	0.04	1.00	1.00	1.00	1.00	1.00	1.00	1.00	0.00	0.30	0.70	1.00	0.01	1.00	1.00	T9	1.00	1.00	1.00	1.00	1.00	1.00
T10	0.03	1.00	1.00	1.00	1.00	1.00	1.00	0.11	0.02	1.00	0.80	1.00	1.00	1.00	1.00	1.00	0.51	0.74	1.00	0.01	1.00	1.00	1.00	1.00	T10	1.00	1.00	1.00	0.75	0.07
T11	1.00	0.02	1.00	1.00	1.00	0.74	1.00	1.00	0.96	1.00	1.00	1.00	0.04	1.00	1.00	0.00	0.00	0.01	0.06	0.00	1.00	1.00	1.00	1.00	0.63	T11	1.00	1.00	1.00
T12	0.00	1.00	0.17	0.69	0.15	1.00	0.06	0.00	0.00	0.29	0.01	1.00	1.00	1.00	0.26	0.04	0.06	1.00	1.00	1.00	0.92	1.00	1.00	1.00	1.00	0.09	T12	1.00	0.39	0.03
T13	0.01	1.00	0.75	1.00	1.00	1.00	0.35	0.02	0.01	0.93	0.13	1.00	1.00	1.00	1.00	0.27	0.01	1.00	1.00	1.00	0.23	1.00	1.00	1.00	1.00	0.59	1.00	T13	1.00	1.00
T14	0.00	1.00	0.02	0.05	0.02	1.00	0.01	0.00	0.00	0.03	0.00	1.00	1.00	1.00	0.05	0.00	1.00	1.00	1.00	1.00	1.00	1.00	0.58	1.00	1.00	0.01	1.00	1.00	T14	1.00
T15	0.00	1.00	0.44	1.00	0.45	1.00	0.18	0.01	0.00	0.58	0.05	1.00	1.00	1.00	0.64	0.15	0.06	1.00	1.00	1.00	0.70	1.00	1.00	1.00	1.00	0.25	1.00	1.00	1.00	T15

Figure 12: P-values (green, < 0.05; blue, >= 0.05) of the Wilcoxon signed ranks tests (Bonferroni-Holm correction) for all comparisons for scratchiness (left) and hairiness (right). The ratings of scratchiness and hairiness were found to significantly differ depending on the sample (scratchiness, $\chi^2(29) = 315.01$, $p < .001$; hairiness, $\chi^2(29) = 394.38$, $p < .001$).

Figure 13 — Uniformity (left) / Isotropy (right)

	R1	R2	R3	R4	R5	R6	R7	R8	R9	R10	R11	R12	R13	R14	R15	T1	T2	T3	T4	T5	T6	T7	T8	T9	T10	T11	T12	T13	T14	T15
R1	R1	1.00	1.00	0.56	1.00	1.00	1.00	1.00	1.00	1.00	1.00	0.76	1.00	1.00	1.00	1.00	0.01	0.21	0.02	1.00	0.00	0.89	0.02	0.42	0.22	1.00	0.08	0.02	0.00	0.07
R2	1.00	R2	1.00	1.00	1.00	1.00	1.00	1.00	1.00	1.00	1.00	1.00	1.00	1.00	1.00	1.00	0.12	1.00	0.25	1.00	0.00	1.00	0.17	1.00	1.00	1.00	1.00	0.00	0.00	1.00
R3	1.00	1.00	R3	1.00	1.00	1.00	1.00	1.00	1.00	1.00	1.00	1.00	1.00	1.00	1.00	1.00	0.03	0.89	0.06	1.00	0.00	1.00	0.04	1.00	0.74	1.00	0.22	0.03	0.00	0.19
R4	1.00	1.00	1.00	R4	1.00	1.00	1.00	1.00	1.00	1.00	1.00	1.00	1.00	1.00	1.00	1.00	1.00	1.00	1.00	1.00	0.21	1.00	1.00	1.00	1.00	1.00	1.00	1.00	1.00	1.00
R5	1.00	1.00	1.00	1.00	R5	1.00	1.00	1.00	1.00	1.00	1.00	1.00	1.00	1.00	1.00	1.00	0.03	1.00	0.05	1.00	0.00	1.00	0.03	1.00	0.59	1.00	0.22	0.02	0.00	0.34
R6	0.11	1.00	1.00	1.00	1.00	R6	1.00	1.00	1.00	1.00	1.00	1.00	1.00	1.00	1.00	1.00	0.85	1.00	1.00	1.00	0.03	1.00	1.00	1.00	1.00	1.00	1.00	1.00	0.36	1.00
R7	1.00	1.00	1.00	1.00	1.00	1.00	R7	1.00	1.00	1.00	1.00	1.00	1.00	1.00	1.00	1.00	0.03	1.00	0.15	1.00	0.00	1.00	0.09	1.00	1.00	1.00	0.50	0.08	0.00	0.67
R8	1.00	1.00	1.00	1.00	1.00	1.00	0.95	R8	1.00	1.00	1.00	1.00	1.00	1.00	1.00	1.00	0.15	1.00	0.50	1.00	0.00	1.00	0.35	1.00	1.00	1.00	0.24	0.01	1.00
R9	1.00	1.00	1.00	1.00	1.00	1.00	1.00	1.00	R9	1.00	1.00	1.00	1.00	1.00	1.00	1.00	0.07	1.00	0.17	1.00	0.00	1.00	0.15	1.00	1.00	1.00	0.66	0.11	0.00	0.66
R10	1.00	1.00	1.00	1.00	1.00	1.00	1.00	1.00	1.00	R10	1.00	1.00	1.00	1.00	1.00	1.00	0.19	1.00	0.90	1.00	0.01	1.00	0.56	1.00	1.00	1.00	0.43	0.02	1.00
R11	1.00	1.00	1.00	1.00	1.00	1.00	1.00	1.00	1.00	1.00	R11	1.00	1.00	1.00	1.00	1.00	0.02	0.77	0.01	1.00	0.00	1.00	0.01	0.58	0.21	1.00	0.07	0.00	0.00	0.09
R12	0.76	1.00	1.00	1.00	1.00	1.00	1.00	1.00	1.00	1.00	1.00	R12	1.00	1.00	1.00	1.00	0.54	1.00	1.00	1.00	0.00	1.00	0.81	1.00	1.00	1.00	0.34	0.01	1.00
R13	1.00	1.00	1.00	1.00	1.00	1.00	1.00	1.00	1.00	1.00	1.00	1.00	R13	1.00	1.00	1.00	1.00	1.00	1.00	1.00	0.08	1.00	1.00	1.00	1.00	1.00	1.00	0.21	1.00
R14	1.00	1.00	1.00	1.00	1.00	1.00	1.00	1.00	1.00	1.00	1.00	1.00	1.00	R14	1.00	1.00	0.05	1.00	0.28	1.00	0.00	1.00	0.15	1.00	1.00	1.00	0.80	0.13	0.00	0.72
R15	1.00	1.00	1.00	1.00	1.00	0.30	1.00	1.00	1.00	1.00	1.00	1.00	1.00	1.00	R15	1.00	0.13	1.00	0.63	1.00	0.00	1.00	0.20	1.00	1.00	1.00	1.00	0.11	0.00	0.72
T1	0.19	1.00	1.00	1.00	1.00	1.00	1.00	1.00	1.00	1.00	1.00	1.00	1.00	1.00	0.30	T1	0.37	1.00	1.00	1.00	0.02	1.00	1.00	1.00	1.00	1.00	1.00	1.00	0.09	1.00
T2	0.00	0.00	0.00	0.00	0.00	0.00	0.00	0.00	0.00	0.00	0.00	0.00	0.00	0.00		0.00	T2	1.00	1.00	1.00	1.00	1.00	1.00	1.00	0.31	1.00	1.00	1.00	1.00	1.00
T3	0.00	0.00	0.02	0.06	0.00	0.07	0.00	0.00	0.00	0.01	0.00	0.03	0.00	0.00		0.83	0.90	T3	1.00	1.00	1.00	1.00	1.00	1.00	1.00	1.00	1.00	1.00	1.00	1.00
T4	0.00	0.00	0.02	0.10	0.01	0.12	0.00	0.00	0.00	0.01	0.01	0.04	0.01	0.00		0.00	0.90	1.00	T4	1.00	1.00	1.00	1.00	1.00	1.00	1.00	1.00	1.00	1.00	1.00
T5	0.00	0.02	0.77	1.00	0.06	1.00	0.03	0.02	0.01	0.08	0.11	1.00	0.08	0.01	0.00	1.00	0.00	1.00	1.00	T5	0.22	1.00	1.00	1.00	1.00	1.00	1.00	1.00	1.00	1.00
T6	0.00	0.00	0.00	0.01	0.00	0.01	0.00	0.00	0.00	0.00	0.00	0.00	0.00	0.00		0.13	1.00	1.00	1.00	0.27	T6	0.31	1.00	0.42	0.18	0.00	1.00	0.53	1.00	1.00
T7	0.21	1.00	1.00	1.00	1.00	1.00	1.00	1.00	0.62	1.00	1.00	1.00	1.00	0.93	0.15	1.00	0.01	1.00	1.00	1.00	0.34	T7	1.00	1.00	1.00	1.00	1.00	1.00	1.00	1.00
T8	0.00	0.01	0.12	0.35	0.02	0.77	0.01	0.01	0.00	0.03	0.03	0.24	0.02	0.01	0.00	1.00	0.03	1.00	1.00	1.00	1.00	1.00	T8	1.00	0.66	1.00	1.00	1.00	1.00	1.00
T9	0.00	0.00	0.03	0.14	0.00	0.22	0.00	0.00	0.00	0.01	0.01	0.08	0.00	0.00		1.00	0.04	1.00	1.00	1.00	1.00	1.00	1.00	T9	1.00	1.00	1.00	1.00	1.00	1.00
T10	0.01	0.06	1.00	1.00	0.25	1.00	0.14	0.08	0.03	0.26	0.73	1.00	0.35	0.04	0.01	1.00	0.00	1.00	1.00	1.00	0.06	1.00	1.00	1.00	T10	1.00	1.00	1.00	1.00	1.00
T11	0.00	0.03	1.00	1.00	0.12	1.00	0.04	0.03	0.01	0.10	0.32	1.00	0.18	0.01	0.00	1.00	0.00	0.26	0.52	1.00	0.01	1.00	1.00	1.00	1.00	T11	0.33	0.01	1.00
T12	0.00	0.00	0.02	0.06	0.00	0.11	0.00	0.00	0.00	0.00	0.04	0.00	0.00	0.00		1.00	0.08	1.00	1.00	1.00	1.00	1.00	1.00	1.00	1.00	1.00	T12	1.00	1.00	1.00
T13	0.00	0.00	0.03	0.10	0.00	0.18	0.00	0.00	0.00	0.01	0.00	0.06	0.00	0.00		1.00	0.03	1.00	1.00	1.00	1.00	1.00	1.00	1.00	1.00	1.00	1.00	T13	1.00	1.00
T14	0.00	0.00	0.00	0.00	0.00	0.00	0.00	0.00	0.00	0.00	0.00	0.00	0.00	0.00		0.07	1.00	1.00	1.00	0.34	1.00	0.30	1.00	1.00	0.05	0.00	1.00	1.00	T14	1.00
T15	0.03	0.34	1.00	1.00	1.00	1.00	0.38	0.20	0.16	0.81	1.00	1.00	1.00	0.21	0.02	1.00	0.00	1.00	1.00	1.00	0.16	1.00	1.00	1.00	1.00	1.00	1.00	1.00	0.13	T15

Figure 13: P-values (green, < 0.05; blue, >= 0.05) of the Wilcoxon signed ranks tests (Bonferroni-Holm correction) for all comparisons for uniformity (left) and isotropy (right). The ratings of uniformity and isotropy were found to significantly differ depending on the sample (uniformity, $\chi^2(29) = 329.88$, $p < .001$; isotropy, $\chi^2(29) = 189.08$, $p < .001$).